Appendix A.40:

Willryan Ave – CPT 2168

Table 1: Site Description for Willryan Ave (CPT 2168).

Attribute	Yes/No			Description/Date	Symbol in Figure 1
	10-m Buffer	20-m Buffer	50-m Buffer		
Near a body of surface water or other free face features?	No	No	No	The center of the site is ~345 m to the NE from the Avon River (the free-face height is ~1.5 m) and ~490 m to the E from Anzac Wetland (the free-face height is ~2 m).	NA
Lateral spreading observed during the CES?	No	No	No	No lateral spreading was observed by the mapping team.[1]	NA
Nearby buildings or structures?	No	Yes	Yes	Building coverage of the 20-m and 50-m buffers is 8% and 24%, respectively. The buildings are in the NW and SW quadrants of the 20-m buffer and all quadrants of the 50-m buffer.	White Fill + Brown Outline
Sloping land?	Yes	Yes	Yes	Residential, predominantly level area except for gently sloping driveways, especially two driveways in the E portion of the 20- and 50-m buffers.	NA
Step changes in the ground surface?	Yes	Yes	Yes	Properties are slightly elevated relative to the road, especially two front lawns in the E portion of the 20-m and 50-m buffer, which are ~0.5 m above the road level.	NA
Retaining walls?	No	Yes	Yes	One front lawn in the E portion of the 20-m and 50-m buffer is retained by an ~0.5-m high wall.	Retaining Wall: Black Line
Vegetation?	Yes	Yes	Yes	Trees and bushes cover 13, 17, and 25% of the 10-, 20-, and 50-m buffers, respectively. They are in all quadrants of the buffers.	White Fill + Green Outline
Anthropogenic changes to the site between the LiDAR surveys?	No	Yes	Yes	Building removal in the E portion of the 50-m buffer between Dec 24, 2011, and Apr 2012. Building addition at the same property in the E portion of the 50-m buffer and building removal in the NW quadrant of the 200- and 50-m buffers between Sep 2013 and Feb 2014. Building removal in the NW quadrant of the 50-m buffer between Feb 2014 and Aug 2014. Building removal in the E portion of the 20- and 50-m buffer between Aug 2014 and Sep 2014.	Building Addition/ Removal: Orange Crossline
Other important factors?	Yes	Yes	Yes	Low-motor-vehicle-volume, two-way roadway (Willryan Ave) occupies 38, 23, and 9% of the 10-, 20-, an d50-m buffers, respectively, and runs in the NE-SW direction through the NE and SE quadrants of the 10- and 20-m buffers and the NE, SE, and SW quadrants of the 50-m buffer.	Road: Gray Fill + Red Outline

Note: Buffer is the area within a circle of a specified radius with CPT investigations done at its center (172.708731°, -43.499905°).

[1] Canterbury Geotechnical Database. (2012). "Observed Ground Crack Locations", Map Layer CGD0400 - 23 July 2012, retrieved July 09, 2018 from https://canterburygeotechnicaldatabase.projectorbit.com/

Figure 1: Site plan with areas where ejecta-induced settlement is considered.

Note 1: Patch A (outlined in red) in the free field was selected for the settlement assessment as an area free of vegetation and structures. Other important factors considered for the patch selection were its proximity to a CPT, a property subjected to addition and/or demolition of a structure, front yard/backyard alterations (e.g., ploughing, rubble, scrap), and aerial distribution of sediment ejecta. In addition, the entire portion of the road within the 50-m buffer was considered for settlement assessment. Roads as hard, relatively flat surfaces provide many ground-classified points. The LiDAR-based settlement analyses for the Sep-10 EQ were not done due to the evident absence of ejecta from Patch A and Road. The Oct 2015 LiDAR survey was not used for the settlement analysis for Patch A due to the anthropogenic changes.

Table 2: LiDAR flight error adjustments, global adjustments for the difference between average LiDAR point elevations and benchmark survey elevations, and vertical tectonic movement adjustments.

	Adjustments (mm)		
Earthquake Event(s)	LiDAR Flight Error	Global Offset[2]	Tectonic Vertical Movement
Sep-10	-100	-3	0
Feb-11	+50	16	-30
Jun-11	0	38	-45
Dec-11	-50	-65	0
CES	-100	-14	-75
Any LiDAR survey affected by ejecta?			No

Note: The negative sign indicates the subtraction from the ground surface subsidence, while the positive sign indicates the addition to the ground surface subsidence.

Table 3a: LiDAR Measurement Error for Patch A.

Surveys	Buffer	Area Averaged Difference Indicating Repeat Measurement Error (mm)	$\sigma^*_{\text{individual LiDAR points}}$ (mm)	%Reduction in σ due to Area Averaging of LiDAR Points
Post Feb 2011: Mar 2011 and May 2011	10-m	ND	59	[147,147]
	20-m	87		
	50-m	87		
Post Dec 2011: Feb 2012 and Oct 2015	10-m	ND	70	[ND,ND]
	20-m	ND		
	50-m	ND		

*Standard deviation; ND = Not determined.

[2] Russell, J., & van Ballegooy, S. (2015). *Canterbury Earthquake Sequence: Increased liquefaction vulnerability assessment methodology*. New Zealand: Tonkin & Taylor Ltd.

Table 3b: LiDAR Measurement Error for Road.

Surveys	Buffer	Area Averaged Difference Indicating Repeat Measurement Error (mm)	$\sigma^*_{\text{individual LiDAR points}}$ (mm)	%Reduction in σ due to Area Averaging of LiDAR Points
Post Feb 2011: Mar 2011 and May 2011	10-m	77	59	[131,134]
	20-m	79		
	50-m	67		
Post Dec 2011: Feb 2012 and Oct 2015	10-m	27	70	[39,41]
	20-m	29		
	50-m	32		

*Standard deviation.

Table 4a: Ground surface subsidence adjustments due to LiDAR measurement error for Patch A.

Earthquake Event(s)	$\sigma_{\text{pre-EQ LiDAR survey}}$ (mm)	$\sigma_{\text{post-EQ LiDAR survey}}$ (mm)	σ_{total} (mm)	Area Average Adjusted σ (mm) **
Sep-10	158	56	134	±198
Feb-11	56	59	59	±87
Jun-11	59	61	62	±92
Dec-11	61	70	87	±128
CES	158	70	124	±184

**Based on the highest %Reduction in Table 3a.

Table 4b: Ground surface subsidence adjustments due to LiDAR measurement error for Road.

Earthquake Event(s)	$\sigma_{\text{pre-EQ LiDAR survey}}$ (mm)	$\sigma_{\text{post-EQ LiDAR survey}}$ (mm)	σ_{total} (mm)	Area Average Adjusted σ (mm) **
Sep-10	158	56	134	±180
Feb-11	56	59	59	±79
Jun-11	59	61	62	±83
Dec-11	61	70	87	±116
CES	158	70	124	±167

**Based on the highest %Reduction in Table 3b.

Table 5a: Raw liquefaction-related ground surface subsidence using original LiDAR points for Patch A.

	Average Ground Surface Subsidence (mm)		
Earthquake Event(s)	10-m Buffer	20-m Buffer	50-m Buffer
Sep-10	ND	ND	ND
Feb-11	ND	88	88
Jun-11	ND	91	91
Dec-11	ND	71	71
CES	ND	ND	ND

Table 5b: Raw liquefaction-related ground surface subsidence using original LiDAR points for Road.

	Average Ground Surface Subsidence (mm)		
Earthquake Event(s)	10-m Buffer	20-m Buffer	50-m Buffer
Sep-10	ND	ND	ND
Feb-11	75	75	57
Jun-11	91	80	78
Dec-11	67	74	71
CES	ND	ND	ND

Table 6a: Corrected liquefaction-related ground surface subsidence using original LiDAR points for Patch A with the calculated adjustments in Table 2.

	Average Calculated Ground Surface Subsidence (mm)		
Earthquake Event(s)	10-m Buffer	20-m Buffer	50-m Buffer
Sep-10	ND	ND	ND
Feb-11	ND	125±75	125±75
Jun-11	ND	84±100	84±100
Dec-11	ND	-44±125	-44±125
CES	ND	ND	ND

Notes: Plus/minus values are same as those in Table 4a, but rounded to the nearest 25 mm; Positive overall values indicate ground surface subsidence, while negative overall values indicate ground surface uplift.

Table 6b: Corrected liquefaction-related ground surface subsidence using original LiDAR points for Road with the calculated adjustments in Table 2.

	Average Calculated Ground Surface Subsidence (mm)		
Earthquake Event(s)	10-m Buffer	20-m Buffer	50-m Buffer
Sep-10	ND	ND	ND
Feb-11	112±75	111±75	93±75
Jun-11	84±75	73±75	71±75
Dec-11	-49±125	-41±125	-44±125
CES	ND	ND	ND

Notes: Plus/minus values are same as those in Table 4b, but rounded to the nearest 25 mm; Positive overall values indicate ground surface subsidence, while negative overall values indicate ground surface uplift.

Table 7a: Corrected liquefaction-related ground surface subsidence for Patch A using LiDAR DEMs.

	Estimated Ground Surface Subsidence (mm)								
	10-m Buffer			20-m Buffer			50-m Buffer		
Earthquake Event(s)	16th %ile	50th %ile	84th %ile	16th %ile	50th %ile	84th %ile	16th %ile	50th %ile	84th %ile
Sep-10	<50	50	50	<50	50	50	<50	50	50
Feb-11	100	150	200	100	150	200	100	150	200
Jun-11	<50	50	50	<50	50	50	<50	50	50
Dec-11	<50	<50	<50	<50	<50	<50	<50	<50	<50
CES	250	300	400	250	300	400	250	300	400

Note: These percentiles are not the exact statistical measures; they indicate the spatial variability of ground surface subsidence.

Table 7b: Corrected liquefaction-related ground surface subsidence for Road using LiDAR DEMs.

	Estimated Ground Surface Subsidence (mm)								
	10-m Buffer			20-m Buffer			50-m Buffer		
Earthquake Event(s)	16th %ile	50th %ile	84th %ile	16th %ile	50th %ile	84th %ile	16th %ile	50th %ile	84th %ile
Sep-10	<50	<50	50	<50	<50	50	<50	<50	50
Feb-11	100	150	150	100	150	200	100	150	200
Jun-11	50	50	50	50	50	50	50	50	50
Dec-11	<50	50	50	<50	50	100	<50	50	100
CES	250	300	350	250	300	350	250	300	350

Note: These percentiles are not the exact statistical measures; they indicate the spatial variability of ground surface subsidence.

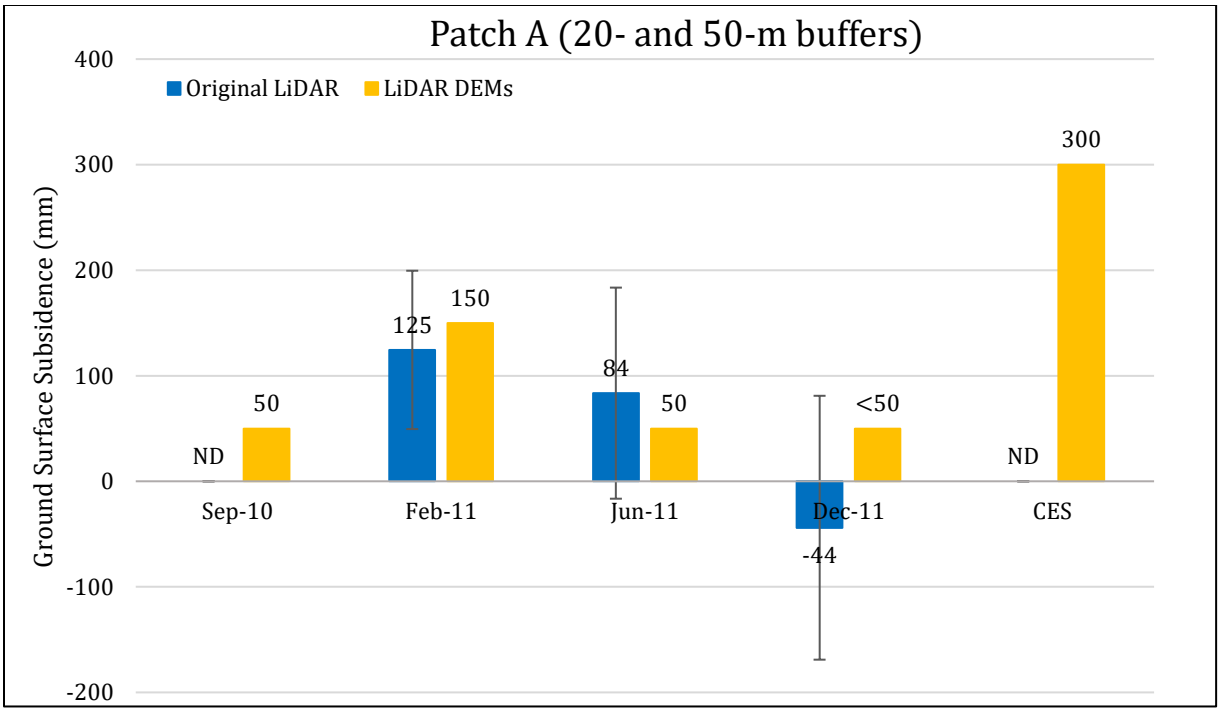

Figure 2: Comparison between ground surface subsidence determined from original LiDAR survey points and ground surface subsidence (50th %ile) estimated using LiDAR DEMs for Patch A.

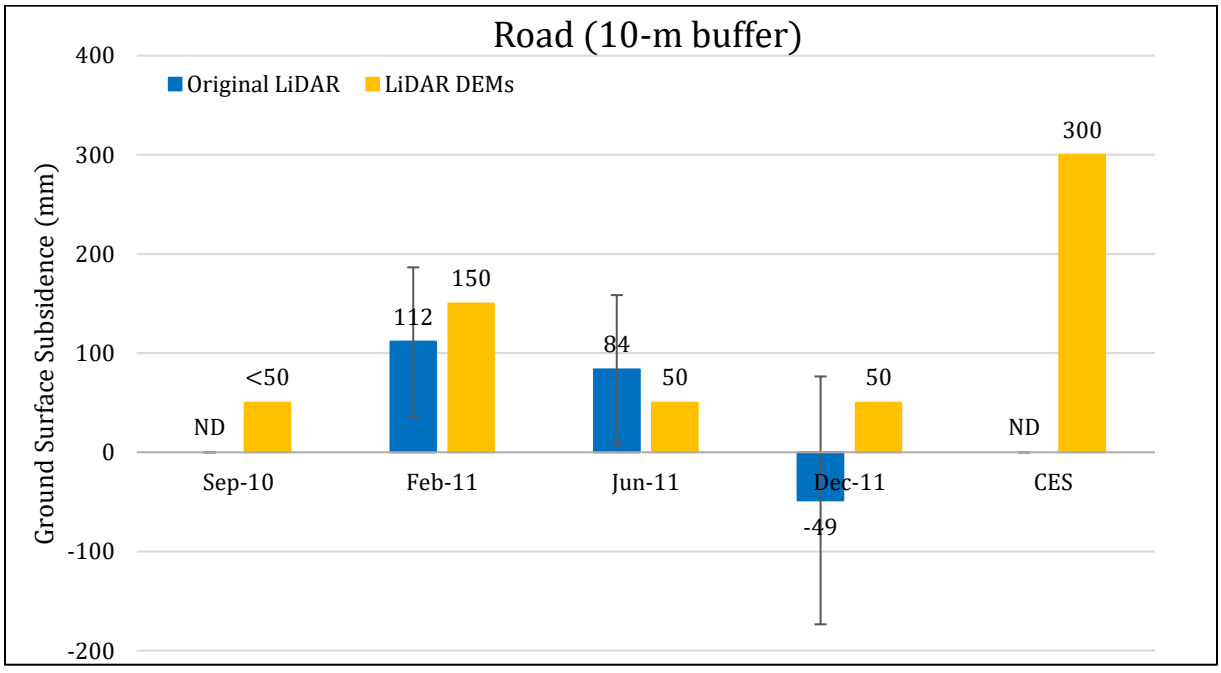

Figure 3: Comparison between ground surface subsidence determined from original LiDAR survey points and ground surface subsidence (50th %ile) estimated using LiDAR DEMs for Road (10-m buffer).

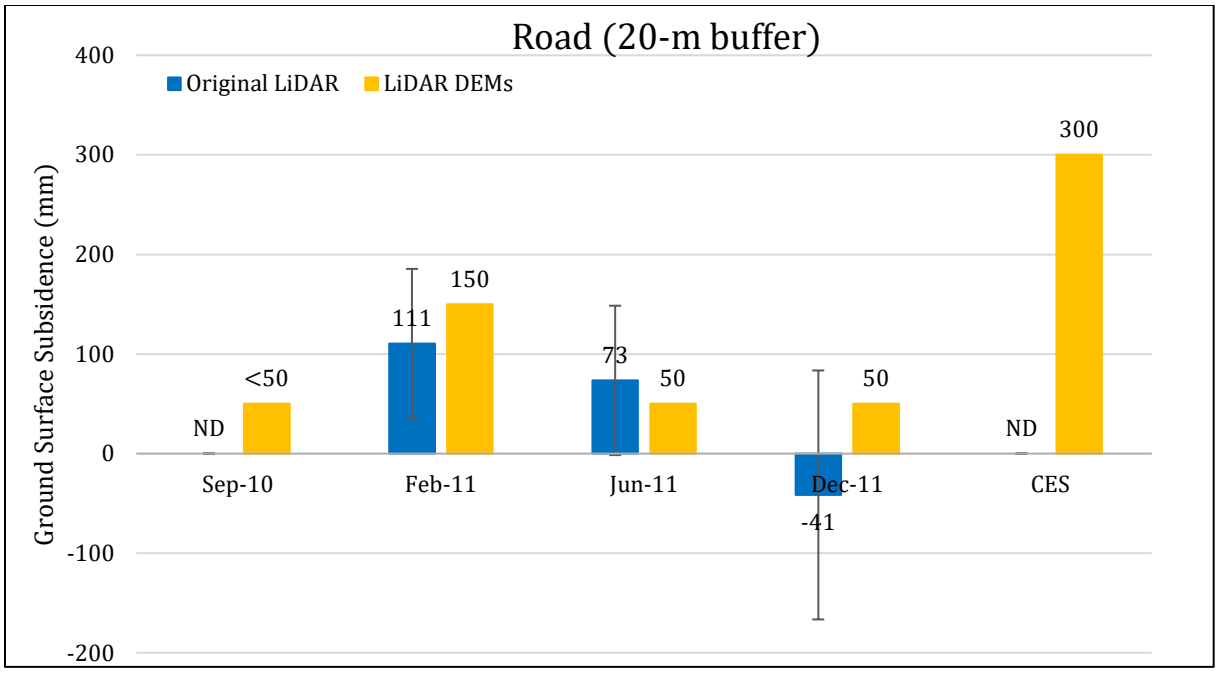

Figure 4: Comparison between ground surface subsidence determined from original LiDAR survey points and ground surface subsidence (50th %ile) estimated using LiDAR DEMs for Road (20-m buffer).

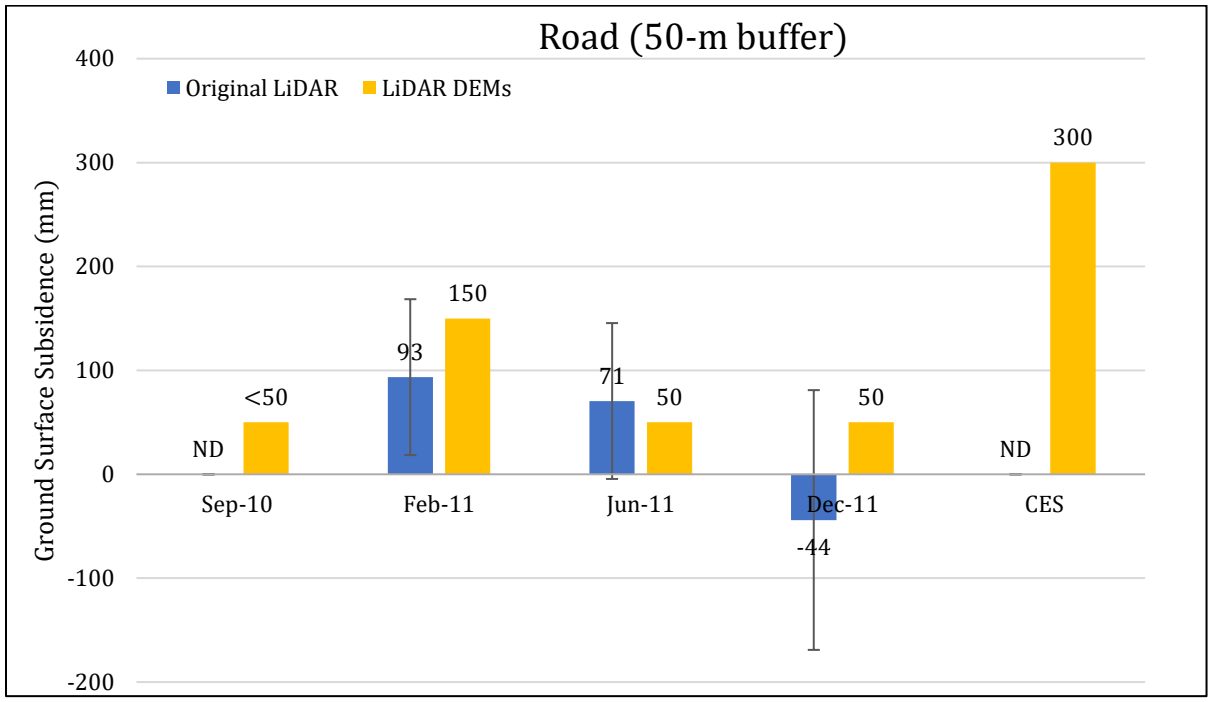

Figure 5: Comparison between ground surface subsidence determined from original LiDAR survey points and ground surface subsidence (50th %ile) estimated using LiDAR DEMs for Road (50-m buffer).

Note 2: The ground surface subsidence values determined using the original LiDAR survey points are consistent with the ground surface subsidence values estimated using the LiDAR DEMs for all earthquake events.

Table 8a: Ejecta-Induced settlement for the top 20 m of the soil profile for Patch A for the 50th %ile PGA, P_L=50%, and C_{FC}=0.13 using BI-2014, ZRB-2002, and I_C cutoff of 2.6.

Earthquake Event(s)	M_W	PGA (g)	Depth to Groundwater (m)	S_T (mm)	S_{V1D} (mm)	$S_{E,L}$ (mm)
Sep-10	7.1	0.17	1.5	ND	12±20	ND
Feb-11	6.2	0.40	1.5	125±75	84±50	41±90
Jun-11	6.2	0.24	1.5	84±100	23±25	61±103
Dec-11	6.1	0.34	0.7	-44±125	81±50	-125±135

Notes: S_T = Total settlement (Table 6); S_{V1D} = Average vertical settlement due to volumetric compression using Boulanger and Idriss (2014) (BI-2014), Zhang et al. (2002) (ZRB-2002) procedures and de Greef and Lengkeek (2018) thin-layer correction; $S_{E,L}$ = Ejecta-induced settlement as the difference between the LiDAR-based S_T and S_{V1D}.

Table 8b: Ejecta-Induced settlement for the top 20 m of the soil profile for Road (10-m buffer) for the 50th %ile PGA, P_L=50%, and C_{FC}=0.13 using BI-2014, ZRB-2002, and I_C cutoff of 2.6.

Earthquake Event(s)	M_W	PGA (g)	Depth to Groundwater (m)	S_T (mm)	S_{V1D} (mm)	$S_{E,L}$ (mm)
Sep-10	7.1	0.17	1.5	ND	12±20	ND
Feb-11	6.2	0.40	1.5	112±75	84±50	28±90
Jun-11	6.2	0.24	1.5	84±75	23±25	61±79
Dec-11	6.1	0.34	0.7	-49±125	81±50	-130±135

Notes: S_T = Total settlement (Table 6); S_{V1D} = Average vertical settlement due to volumetric compression using Boulanger and Idriss (2014) (BI-2014), Zhang et al. (2002) (ZRB-2002) procedures and de Greef and Lengkeek (2018) thin-layer correction; $S_{E,L}$ = Ejecta-induced settlement as the difference between the LiDAR-based S_T and S_{V1D}.

Table 8c: Ejecta-Induced settlement for the top 20 m of the soil profile for Road (20-m buffer) for the 50th %ile PGA, P_L=50%, and C_{FC}=0.13 using BI-2014, ZRB-2002, and I_c cutoff of 2.6.

Earthquake Event(s)	M_W	PGA (g)	Depth to Groundwater (m)	S_T (mm)	S_{V1D} (mm)	$S_{E,L}$ (mm)
Sep-10	7.1	0.17	1.5	ND	12±20	ND
Feb-11	6.2	0.40	1.5	111±75	65±50	46±90
Jun-11	6.2	0.24	1.5	73±75	21±25	52±79
Dec-11	6.1	0.34	0.7	-41±125	63±50	-104±135

Notes: S_T = Total settlement (Table 6); S_{V1D} = Average vertical settlement due to volumetric compression using Boulanger and Idriss (2014) (BI-2014), Zhang et al. (2002) (ZRB-2002) procedures and de Greef and Lengkeek (2018) thin-layer correction; $S_{E,L}$ = Ejecta-induced settlement as the difference between the LiDAR-based S_T and S_{V1D}.

Table 8d: Ejecta-Induced settlement for the top 20 m of the soil profile for Road (50-m buffer) for the 50th %ile PGA, P_L=50%, and C_{FC}=0.13 using BI-2014, ZRB-2002, and I_c cutoff of 2.6.

Earthquake Event(s)	M_W	PGA (g)	Depth to Groundwater (m)	S_T (mm)	S_{V1D} (mm)	$S_{E,L}$ (mm)
Sep-10	7.1	0.17	1.5	ND	13±20	ND
Feb-11	6.2	0.40	1.5	93±75	82±50	11±90
Jun-11	6.2	0.24	1.5	71±75	25±25	46±79
Dec-11	6.1	0.34	0.7	-44±125	80±50	-124±135

Notes: S_T = Total settlement (Table 6); S_{V1D} = Average vertical settlement due to volumetric compression using Boulanger and Idriss (2014) (BI-2014), Zhang et al. (2002) (ZRB-2002) procedures and de Greef and Lengkeek (2018) thin-layer correction; $S_{E,L}$ = Ejecta-induced settlement as the difference between the LiDAR-based S_T and S_{V1D}.

Note 3: The uncertainty for volumetric settlement was derived based on the sensitivity of volumetric settlement to PGA, C_{FC}, and P_L for each earthquake event for VsVp 57203 *Shirley Intermediate School* and CC LIQ 1 – CPT 5586 – *Vivian St* sites. Taking the 50th percentile as the baseline case, the minimum and maximum values corresponding to the difference between the 25th percentile and the 50th percentile and the 75th percentile and the 50th percentile were determined. The arithmetic mean of the range of the minimum and maximum difference was evaluated for each patch at the two sites. The maximum arithmetic mean for each earthquake event was rounded to the nearest five and used as the uncertainty value. Accordingly, the 1-D volumetric settlement uncertainties of ±20, ±50, ±25, and ±50 mm for the Sep-10, Feb-11, Jun-11, and Dec-11 earthquake events, respectively, were used for all sites in this study.

Table 9a: Coverage area and height of ejecta estimates for Patch A (10-, 20-, and 50-m buffers) using photographs.

EQ Event	$H_{E,thick1}$ (mm)	$A_{E,thick1}$ (m^2)	$H_{E,thick2}$ (mm)	$A_{E,thick2}$ (m^2)	$H_{E,thin1}$ (mm)	$A_{E,thin1}$ (m^2)	$H_{E,thin2}$ (mm)	$A_{E,thin2}$ (m^2)	A_T (m^2)
Sep-10	0	0	0	0	0	0	0	0	91.9
Feb-11	100-200	1.7	60-80	60.8	30-50	26.6	5-10	1.9	91.9
Jun-11	0	0	0	0	30-50	55.7	0	0	91.9
Dec-11	0	0	0	0	30-60	11.3	0	0	91.9

Notes: $A_{E,thin/thick}$ = Coverage area of thin/thick ejecta layers; $H_{E,\ thin/thick}$ = Lower-upper estimate of height of thin/thick ejecta layers; A_T= Total assessment area of a buffer being considered.

Table 9b: Coverage area and height of ejecta estimates for Road (10-m buffer) using photographs.

EQ Event	$H_{E,prism/pyr}$ (mm)	$V_{E,prism+pyr}$ (m^3)	$H_{E,thin}$ (mm)	$A_{E,thin}$ (m^2)	A_T (m^2)
Sep-10	0	0	0	0	127
Feb-11	32-200	4.69-6.24	3-6	36.2	127
Jun-11	19-200	2.70-3.73	3-6	74.0	133
Dec-11	15-200	2.84-3.64	5-10	0.5	133

Notes: $H_{E,prism/pyr}$ = Lower-upper estimate of ejecta height near the curb based on 2-4% cross slope of normal crown; $V_{E,prism+pyr}$ = Lower-upper estimate of total volume of prismatic- and pyramidal-shape ejecta; $A_{E,thin}$ =Coverage area of thin ejecta layers; $H_{E,\ thin}$ = Lower-upper estimate of height of thin ejecta layers; A_T= Total assessment area of a buffer being considered.

Table 9c: Coverage area and height of ejecta estimates for Road (20-m buffer) using photographs.

EQ Event	$H_{E,t.prism1}$ (mm)	$H_{E,t.prism2}$ (mm)	$V_{E,t.prism}$ (m^3)	$H_{E,prism/pyr}$ (mm)	$V_{E,prism+pyr}$ (m^3)	$H_{E,thin}$ (mm)	$A_{E,thin}$ (m^2)	A_T (m^2)
Sep-10	0	0	0	0	0	0	0	301
Feb-11	200-300	20-40	3.16-4.89	20-200	7.68-12.3	3-6	89.2	301
Jun-11	0	0	0	9-200	5.68-8.02	3-6	171	303
Dec-11	80-180	20-40	4.46-6.24	13-200	3.27-4.65	5-10	18.7	303

Notes: $H_{E,t.prism1}$ = Lower-upper estimate of ejecta height near the curb based on 2-4% cross slope of normal crown; $H_{E,t.prism2}$ = Lower-upper estimate of ejecta height near the centerline based on 2-4% cross slope of normal crown; $V_{E,t.prism}$ = Lower-upper estimate of total volume of trapezoidal-prism ejecta; $H_{E,prism/pyr}$ = Lower-upper estimate of ejecta height near the curb based on 2-4% cross slope of normal crown; $V_{E,prism+pyr}$ = Lower-upper estimate of total volume of prismatic- and pyramidal-shape ejecta; $A_{E,thin}$ =Coverage area of thin ejecta layers; $H_{E,thin}$ = Lower-upper estimate of height of thin ejecta layers; A_T= Total assessment area of a buffer being considered.

Table 9d: Coverage area and height of ejecta estimates for Road (50-m buffer) using photographs.

EQ Event	$H_{E,t.prism1}$ (mm)	$H_{E,t.prism2}$ (mm)	$V_{E,t.prism}$ (m^3)	$H_{E,prism/pyr}$ (mm)	$V_{E,prism+pyr}$ (m^3)	$H_{E,thin}$ (mm)	$A_{E,thin}$ (m^2)	$H_{E,thick}$ (mm)	$A_{E,thick}$ (m^2)	A_T (m^2)
Sep-10	0	0	0	0	0	0	0	0	0	779
Feb-11	80-300	20-40	11.2-18.2	20-300	17.6-25.9	3-6	260	20-40	6.7	779
Jun-11	ND	ND	ND	ND	ND	ND	ND	ND	ND	779
Dec-11	ND	ND	ND	ND	ND	ND	ND	ND	ND	779

Notes: $H_{E,t.prism1}$ = Lower-upper estimate of ejecta height near the curb based on 2-4% cross slope of normal crown; $H_{E,t.prism2}$ = Lower-upper estimate of ejecta height near the centerline based on 2-4% cross slope of normal crown; $V_{E,t.prism}$ = Lower-upper estimate of total volume of trapezoidal-prism ejecta; $H_{E,prism/pyr}$ = Lower-upper estimate of ejecta height near the curb based on 2-4% cross slope of normal crown; $V_{E,prism+pyr}$ = Lower-upper estimate of total volume of prismatic- and pyramidal-shape ejecta; $A_{E,thin/thick}$ =Coverage area of thin/thick ejecta layers; $H_{E,\ thin/thick}$ = Lower-upper estimate of height of thin/thick ejecta layers; A_T= Total assessment area of a buffer being considered; ND = Not determined due to the uncertainties associated with the shadows and the origin of ejecta.

Note 4: The values in Table 9 correspond to the coverage area of ejecta outlined in aerial photographs (Figures 24 and 73-75) and the lower and upper estimates of ejecta height based on geometrical approximations, ground photographs (Figures 77 and 78), and EQC LDAT property inspection reports (Figure 76). The ejecta-induced settlement using photographs and engineering judgment, $S_{E,P}$, is estimated as

$$
\begin{aligned}
&S_{E,P} \\
&= \frac{\sum_{i=1}^{a} A_{E,thick,i} * H_{E,thick,i} + \sum_{j=1}^{b} A_{E,thin,j} * H_{E,thin,j}}{A_T} \\
&+ \frac{\sum_{l=1}^{d} \left(H_{E,t.prism1,l} + H_{E,t.prism2,l}\right) * W_{E,t.prism,l} * L_{E,t.prism,l}\right)}{A_T} \\
&+ \frac{\frac{1}{2}\sum_{n=1}^{f} W_{E,prism,n} * H_{E,prism,n} * L_{E,prism,n}}{A_T} + \frac{\frac{1}{3}\sum_{p=1}^{g} W_{E,r.pyramid,p} * H_{E,r.pyramid,p} * L_{E,r.pyramid,p}}{A_T} \\
&+ \frac{\frac{1}{6}\sum_{r=1}^{h} W_{E,t.pyramid,r} * H_{E,t.pyramid,r} * L_{E,t.pyramid,r}}{A_T} \\
&= \frac{\sum_{i=1}^{a} V_{E,thick,i} + \sum_{j=1}^{b} V_{E,thin,j} + \sum_{n=1}^{f} V_{E,prism,n} + \sum_{p=1}^{g} V_{E,r.pyramid,p} + \sum_{r=1}^{h} V_{E,t.pyramid,r}}{A_T}
\end{aligned}
$$

where

- $A_{E,thick,i}$ and $H_{E,thick,i}$ are the area and the height of a thick ejecta layer, respectively;
- $A_{E,thin,j}$ and $H_{E,thin,j}$ are the area and the height of a thin ejecta layer, respectively;
- $W_{E,t.prism,l}$ and $L_{E,t.prism,l}$ are the width and the length, respectively, of the coverage area of an ejecta layer shaped as a trapezoidal prism, and $H_{E,t.prism,1/2}$ is the height (base) of the trapezoidal prism-like ejecta layer;
- $A_{E,cone,m}$ and $H_{E,cone,m}$ are the aerea and the height of a conically shaped ejecta, respectively;
- $W_{E,prism,n}$ and $L_{E,prism,n}$ are the width and the length of the coverage area of a prismatically shaped ejecta layer, respectively, and $H_{E,prism,n}$ is the height of a prism-like ejecta layer;

- $W_{E,pyr,p}$ and $L_{E,pyr,p}$ are the width and the length of the coverage area of a pyramid-like ejecta layer, respectively, and $H_{E,pyr,p}$ is the height of a pyramid-like ejecta layer;
- A_T is the total assessment area for a buffer being considered (Figure 1).

Table 10a: Ejecta-induced settlement estimates for Patch A based on photographs.

Earthquake Event	Patch A (10-, 20-, and 50-m buffers)	
	$S_{E,P,lower}$ (mm)	$S_{E,P,upper}$ (mm)
Sep-10	0	0
Feb-11	50	71
Jun-11	18	30
Dec-11	4	7

Note: $S_{E,P,lower}$ and $S_{E,P,upper}$ correspond to lower and upper estimates of $S_{E,P}$, respectively.

Table 10b: Ejecta-induced settlement estimates for Road based on photographs.

Earthquake Event	Road (10-m buffer)		Road (20-m buffer)		Road (50-m buffer)	
	$S_{E,P,lower}$ (mm)	$S_{E,P,upper}$ (mm)	$S_{E,P,lower}$ (mm)	$S_{E,P,upper}$ (mm)	$S_{E,P,lower}$ (mm)	$S_{E,P,upper}$ (mm)
Sep-10	0	0	0	0	0	0
Feb-11	38	51	37	59	38	59
Jun-11	20	28	20	30	ND	ND
Dec-11	21	27	26	37	ND	ND

Note: $S_{E,P,lower}$ and $S_{E,P,upper}$ correspond to lower and upper estimates of $S_{E,P}$, respectively; ND = Not determined due to the uncertainties associated with the shadows and the origin of ejecta.

Table 11a: Best final estimates of ejecta-induced settlement for Patch A.

EQ Event	Patch A (10-, 20-, and 50-m buffers)		
	$S_{E,L}$ (mm)	$S_{E,P}$ (mm)	$S_{E,final}$ (mm)
Sep-10	ND	0	0
Feb-11	41±90	61±10	55±30
Jun-11	61±103	24±6	35±35
Dec-11	-125±135	5.5±1.5	5±5

Notes: $S_{E,L}$ = Ejecta-induced settlement based on LiDAR data reported in Table 8; $S_{E,P}$ = Median ejecta-induced settlement for the range of values reported in Table 10; $S_{E,final}$ = Best final estimate of ejecta-induced settlement rounded to the nearest 5 mm; Final plus/minus values are also rounded to the nearest 5 mm; ND = Not determined.

Table 11b: Best final estimates of ejecta-induced settlement for Road.

EQ Event	Road (10-m buffer)			Road (20-m buffer)			Road (50-m buffer)		
	$S_{E,L}$ (mm)	$S_{E,P}$ (mm)	$S_{E,final}$ (mm)	$S_{E,L}$ (mm)	$S_{E,P}$ (mm)	$S_{E,final}$ (mm)	$S_{E,L}$ (mm)	$S_{E,P}$ (mm)	$S_{E,final}$ (mm)
Sep-10	ND	0	0	ND	0	0	ND	0	0
Feb-11	28±90	45±6	40±30	46±90	48±11	45±30	11±90	49±10	35±30
Jun-11	61±79	24±4	35±25	52±79	25±5	35±25	46±79	ND	*45±80
Dec-11	-130±135	24±3	25±5	-104±135	32±5	30±5	-124±135	ND	ND

Notes: $S_{E,L}$ = Ejecta-induced settlement based on LiDAR data reported in Table 8; $S_{E,P}$ = Median ejecta-induced settlement for the range of values reported in Table 10; $S_{E,final}$ = Best final estimate of ejecta-induced settlement rounded to the nearest 5 mm; Final plus/minus values are also rounded to the nearest 5 mm; ND = Not determined; * indicates low confidence due to the unavailability of $S_{E,P}$.

Note 5:

- Patch A: $S_{E,final}$ for the Sep-10 and Dec-11 EQs is based solely on $S_{E,P}$ due to the evident absence of ejecta for the Sep-10 EQ and the negative $S_{E,L}$ values for the Dec-11 EQ. $S_{E,final}$ for the Feb-11 and Jun-11 EQs is the weighted average of $S_{E,L}$ and $S_{E,P}$ with weights of 1/3 and 2/3, respectively. The uncertainty associated with $S_{E,final}$ is also the weighted average of uncertainties associated with $S_{E,L}$ and $S_{E,P}$ with the same respective weights of 1/3 and 2/3.
- Road (10-m and 20-m buffers): $S_{E,final}$ for the Sep-10 and Dec-11 EQs is based solely on $S_{E,P}$ due to the evident absence of ejecta for the Sep-10 EQ and the negative $S_{E,L}$ for the Dec-11 EQ. $S_{E,final}$ for the Feb-11 and Jun-11 EQs is the weighted average of $S_{E,L}$ and $S_{E,P}$ with weights of 1/3 and 2/3, respectively. The uncertainty associated with $S_{E,final}$ is also the weighted average of uncertainties associated with $S_{E,L}$ and $S_{E,P}$ with the same respective weights of 1/3 and 2/3.
- Road (50-m buffer): $S_{E,final}$ for the Sep-10 EQ is based solely on $S_{E,P}$ due to the evident absence of ejecta. $S_{E,final}$ for the Dec-11 EQ could not be determined due to the negative $S_{E,L}$ and the unavailability of $S_{E,P}$ (due to partial ejecta removal). $S_{E,final}$ for the Feb-11 EQ is the weighted average of $S_{E,L}$ and $S_{E,P}$ with weights of 1/3 and 2/3, respectively. The uncertainty associated with $S_{E,final}$ is also the weighted average of uncertainties associated with $S_{E,L}$ and $S_{E,P}$ with the same respective weights of 1/3 and 2/3. $S_{E,final}$ for the Jun-11 EQ is based solely on $S_{E,L}$ due to the unavailability of $S_{E,P}$ (it could not be determined because of the shadows and unknown origins of the ejecta piles).
- The weight coefficients are based on the LiDAR error bands, LPI prediction error (Maurer et al. 2014[3]), presence of ejecta at the time of LiDAR surveys, discrepancy between the LiDAR-based estimates of ejecta-induced settlement and the quantum of ejecta visible on the aerial photographs, and completeness of visual evidence (i.e., ground and aerial photographs and EQC LDAT property inspection reports for the site). The Willryan Ave site is in the apparent zone of higher ground surface subsidence for the Sep-10 EQ (i.e., the Jul-03 and Sep-10 LiDAR flight errors) and the apparent zone of lower ground surface subsidence for the Feb-11 EQ (i.e., the Sep-10 LiDAR flight error). The site is in the zone of accurate LPI prediction of liquefaction severity for the Sep-10 and Feb-11 EQs. The LDAT inspection report and ground

[3] Maurer, B. W., Green, R. A., Cubrinovski, M., & Bradley, B. A. (2014). Evaluation of the Liquefaction Potential Index for Assessing Liquefaction Hazard in Christchurch, New Zealand. *Journal of Geotechnical and Geoenvironmental Engineering*, 140(7), 04014032-1-11. doi:10.1061/(asce)gt.1943-5606.0001117

photographs from 2 June 2011 are available for the property with Patch A; however, no ejecta height measurements were taken. The ground photographs showing the ejecta remnants at other properties within the 50-m buffer are available, but the ejecta height was not measured. There are no ground photographs of the road.

Summary 1:

- **The best estimate of the ejecta-induced free-field ground settlement at the Willryan Ave site for the SEP 2010, FEB 2011, JUN 2011, and DEC 2011 earthquake is 0 mm, 55±30 mm, 35±35 mm, and 5±5 mm, respectively.**
- **The best estimate of the ejecta-induced free-field ground settlement of the road at the Willryan Ave site for the SEP 2010, FEB 2011, JUN 2011, and DEC 2011 earthquake is 0 mm, 45±30 mm, 35±25 mm, and 30±5 mm, respectively.**

Figure 6: Location of the site.

Figure 7: Position of the site relative to nearby buildings, vegetation, and free-face features.

Figure 8: Street view of the flat land.

Figure 9: Street view of the retaining wall and slightly sloping driveways.

Figure 10: Satellite image of the site taken in Dec 2004.

Figure 11: Satellite image of the site taken in Mar 2009.

Figure 12: Satellite image of the site taken on Sep 3, 2010.

Figure 13: Satellite image of the site taken on Sep 5, 2010.

Figure 14: Satellite image of the site taken on Feb 7, 2011.

Figure 15: Satellite image of the site taken on Feb 23, 2011.

Figure 16: Satellite image of the site taken on Feb 26, 2011.

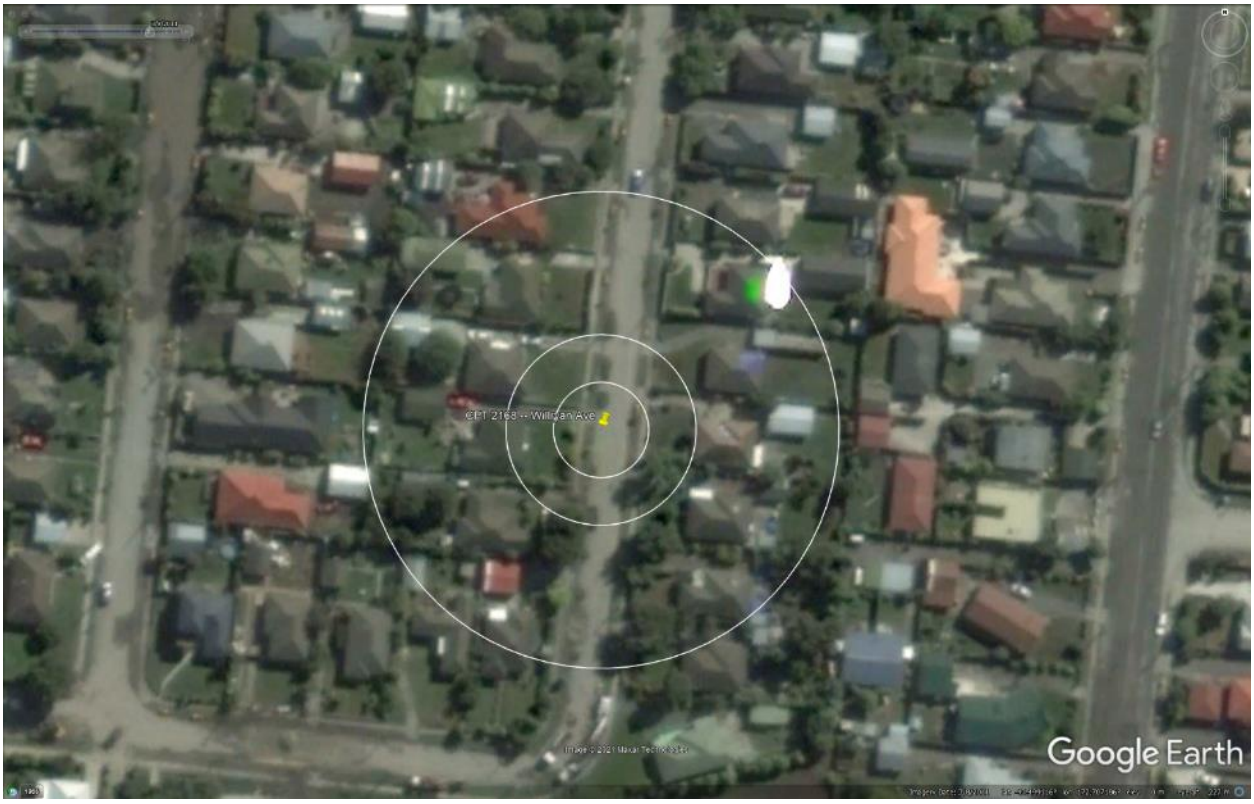

Figure 17: Satellite image of the site taken on Mar 8, 2011.

Figure 18: Satellite image of the site taken in Apr 2012.

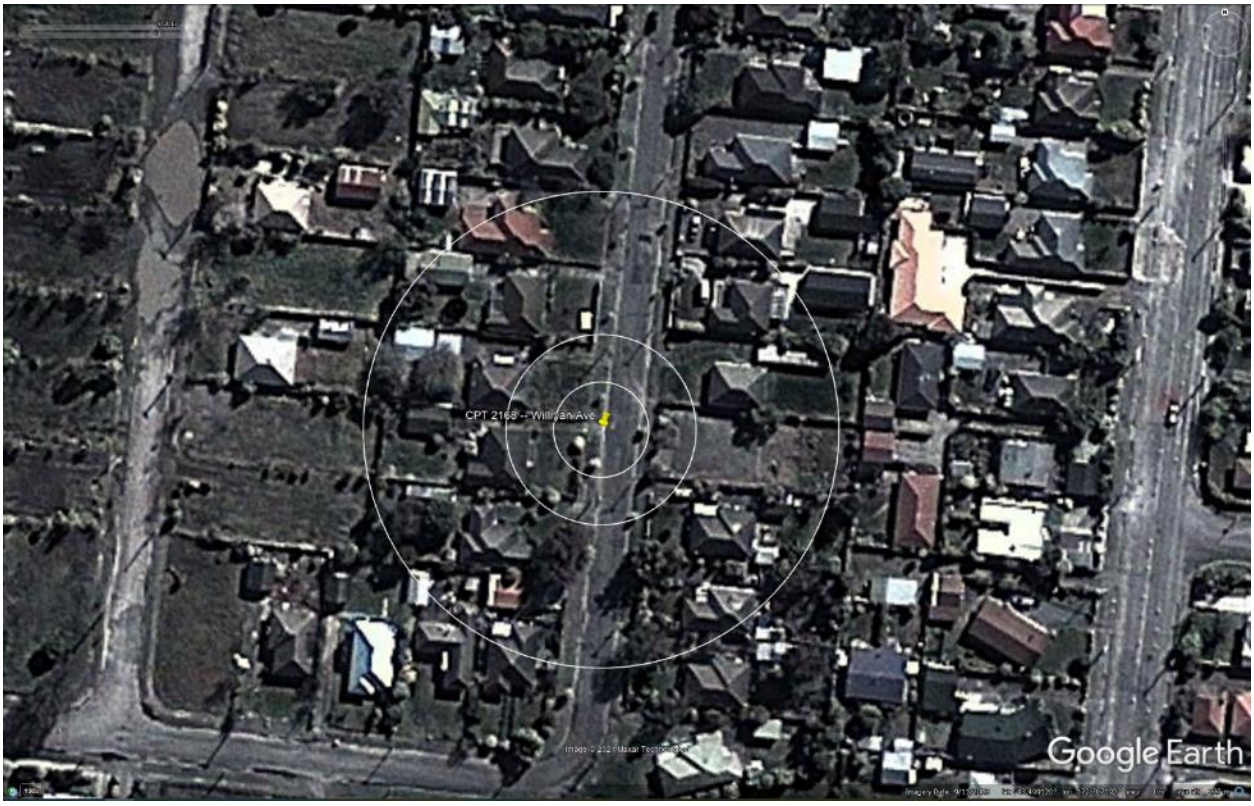

Figure 19: Satellite image of the site taken in Sep 2013.

Figure 20: Satellite image of the site taken in Feb 2014.

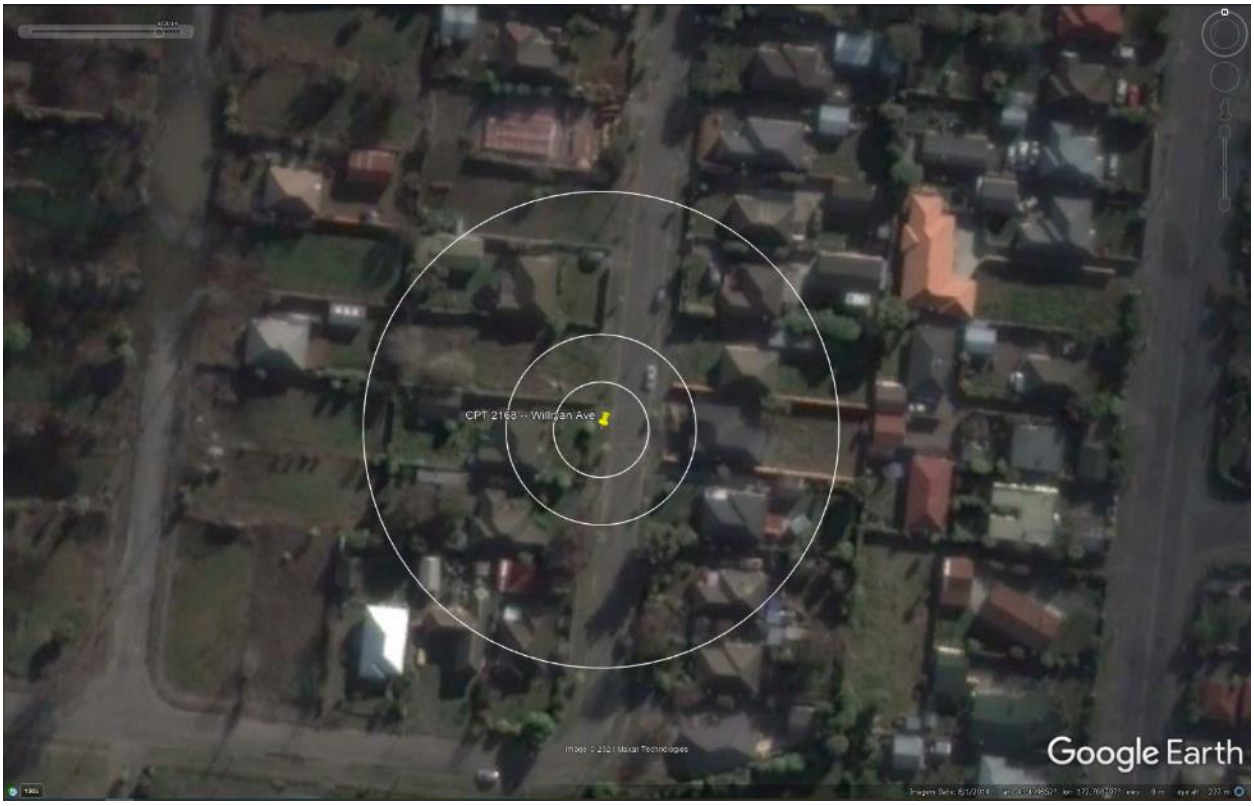

Figure 21: Satellite image of the site taken in Aug 2014.

Figure 22: Satellite image of the site taken in Sep 2014.

Figure 23: Satellite image of the site taken in Nov 2015.

Figure 24: Aerial photograph of the site taken on Sep 4, 2010.

Figure 25: Aerial photograph of the site taken on Feb 24, 2011.

Figure 26: Aerial photograph of the site taken on June 14-15, 2011.

Figure 27: Aerial photograph of the site taken on June 16, 2011.

Figure 28: Aerial photograph of the site taken on Dec 24, 2011.

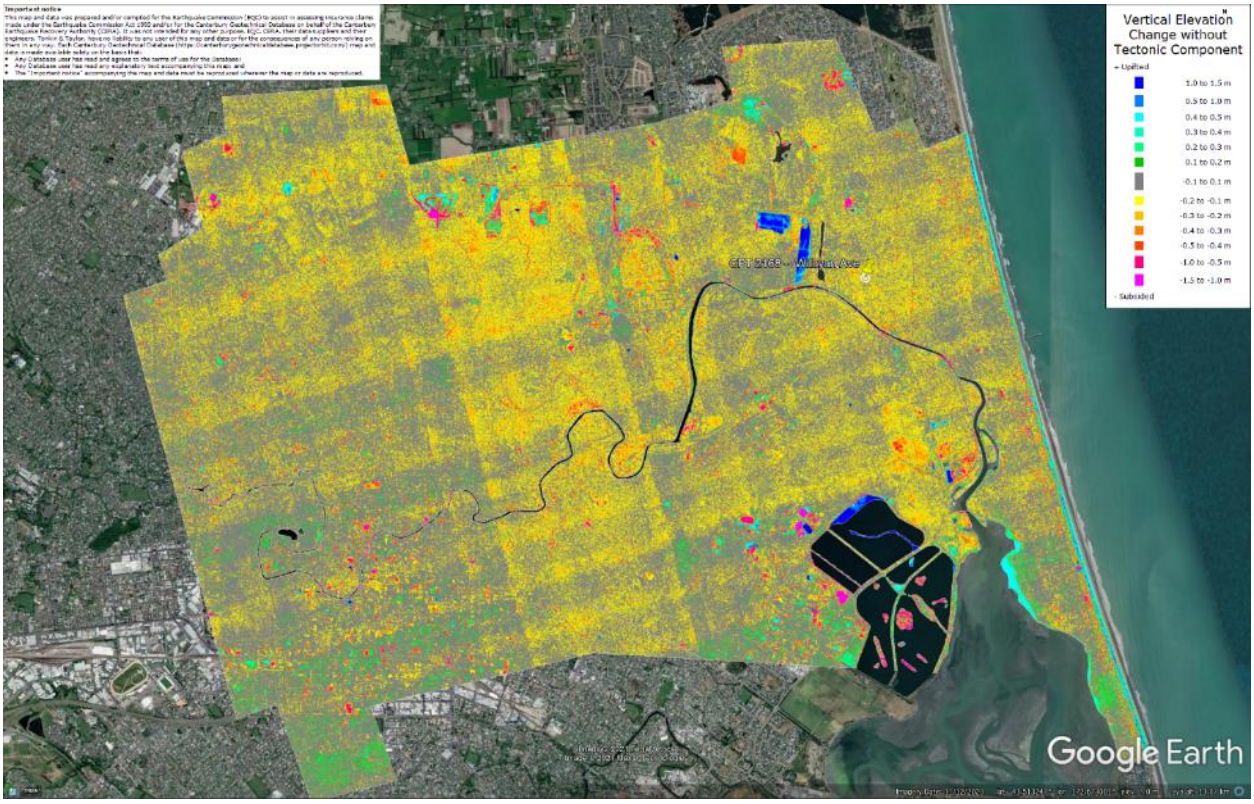

Figure 29: Vertical Ground Movements (Surface – Tectonic) for Sep 2010 Earthquake – the site is in the apparent zone of overestimated ground surface subsidence (i.e., July 2003 and Sep 2010 LiDAR flight error bands).

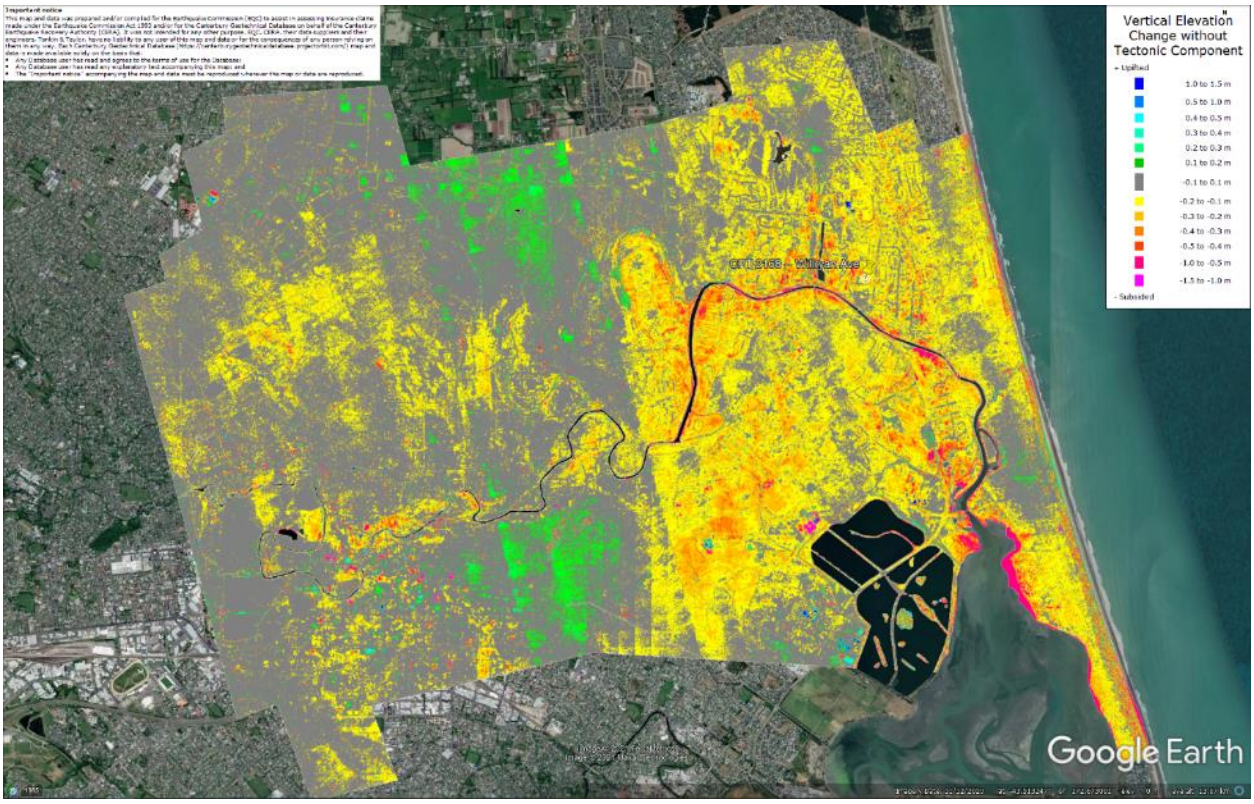

Figure 30: Vertical Ground Movements (Surface – Tectonic) for Feb 2011 Earthquake – the site is not in the apparent zone of underestimated ground surface subsidence (i.e., Sep 2010 LiDAR flight band error).

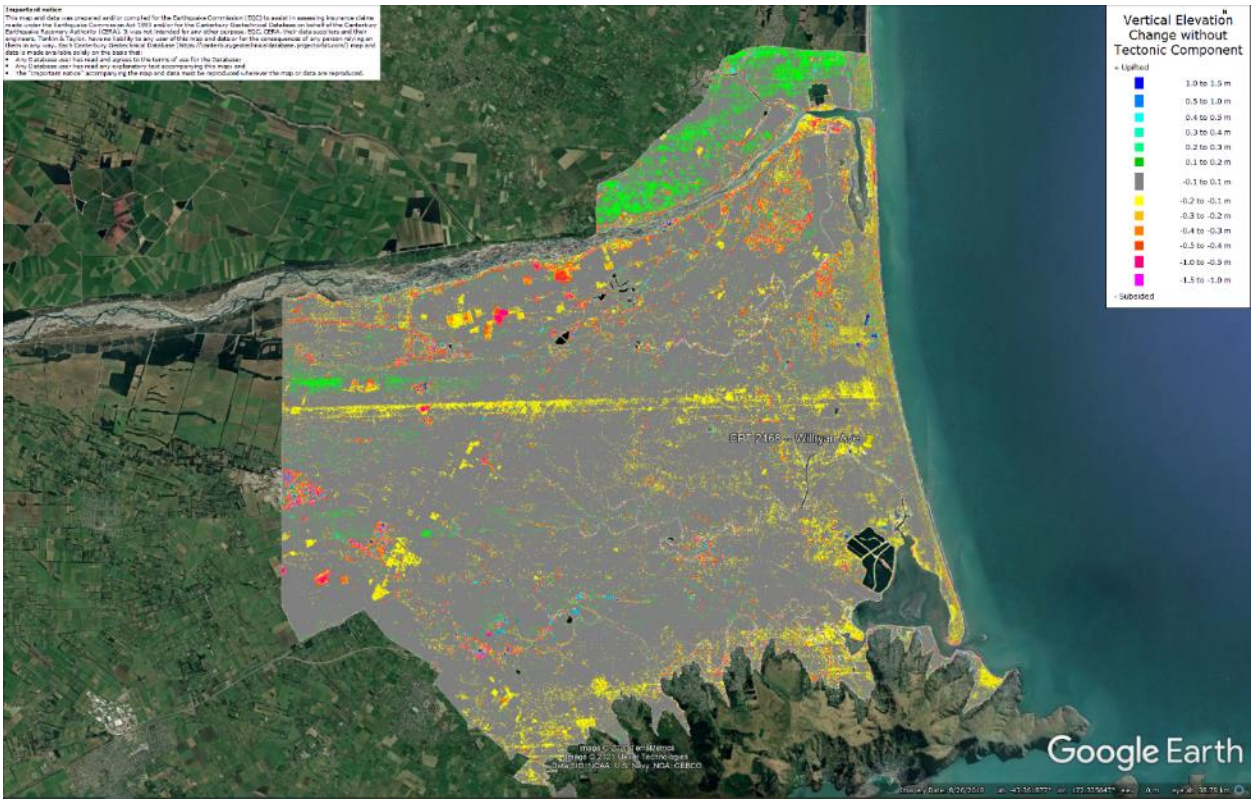

Figure 31: Vertical Ground Movements (Surface – Tectonic) for June 2011 Earthquake – the site is not in the apparent zone of overestimated or underestimated ground surface subsidence.

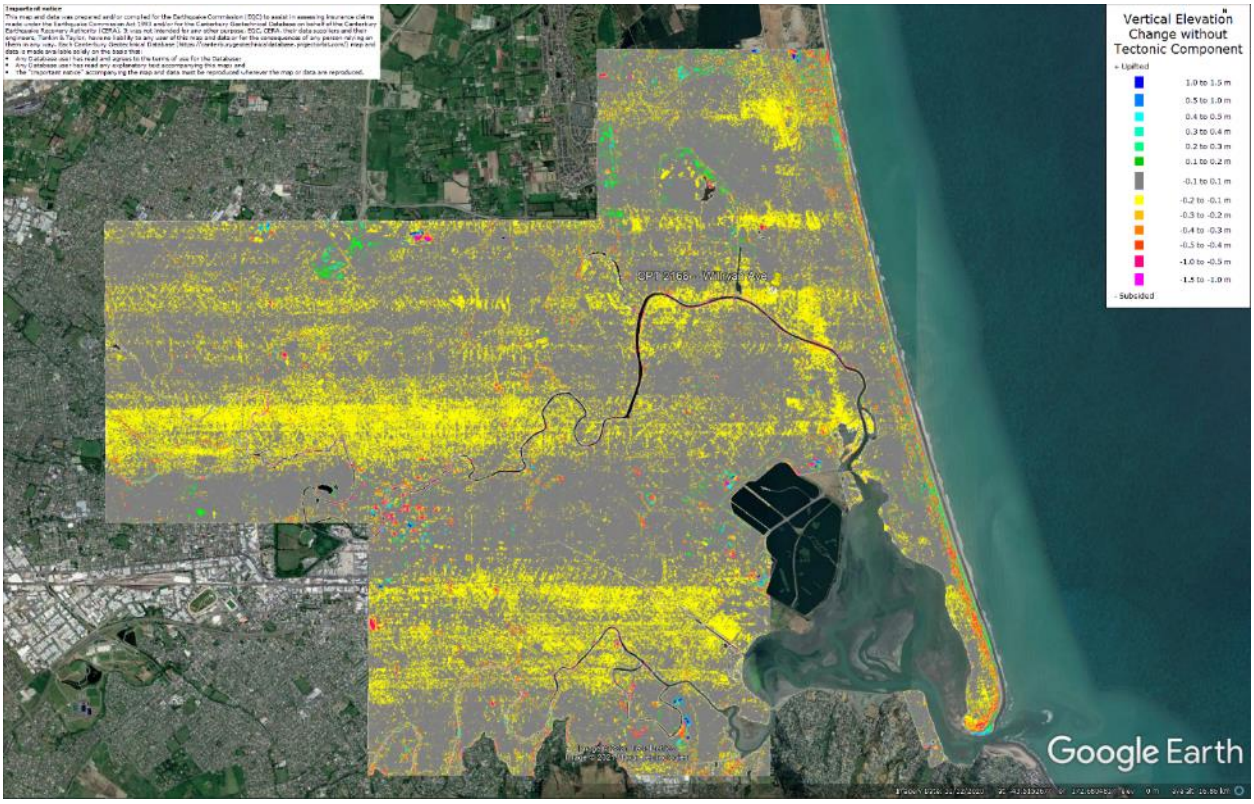

Figure 32: Vertical Ground Movements (Surface – Tectonic) for Dec 2011 Earthquake – the site is in the apparent zone of overestimated ground surface subsidence (i.e., Feb 2012 LiDAR flight band error).

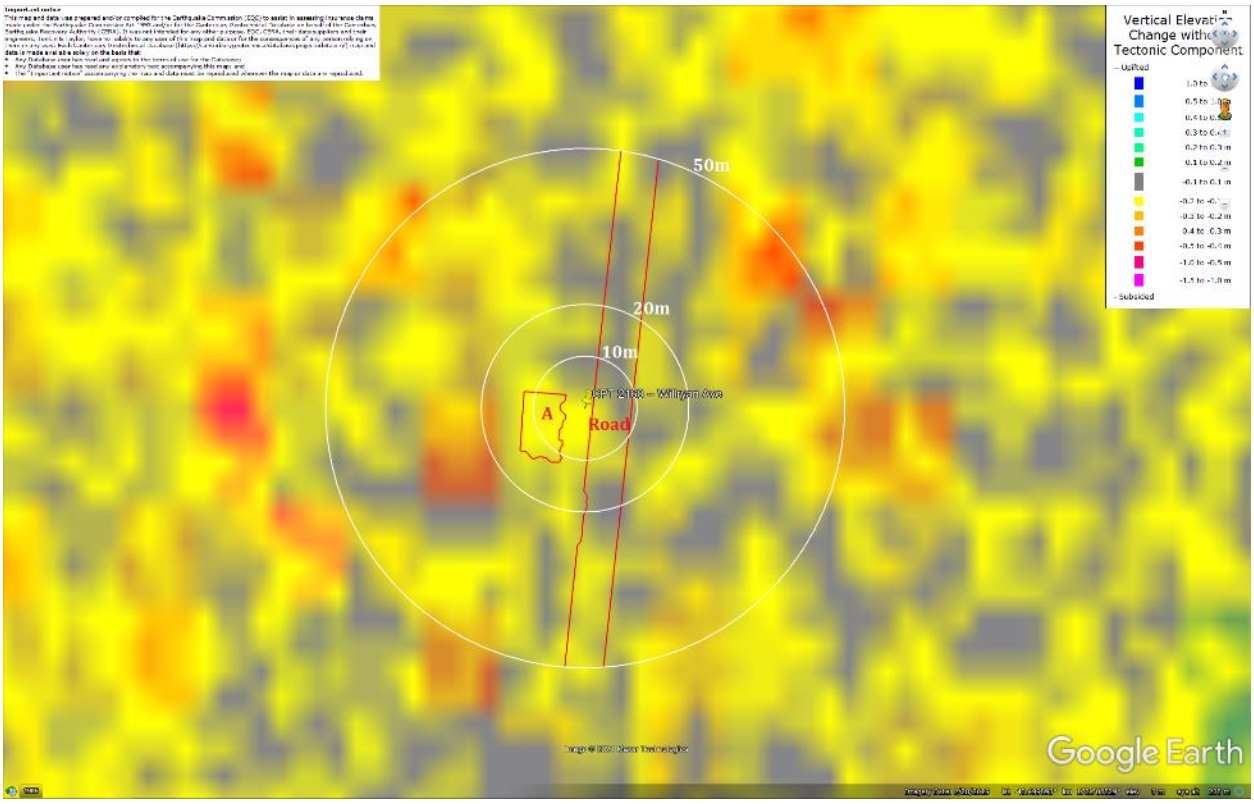

Figure 33: Ground surface subsidence without tectonic component for Sep 2010 Earthquake according to the LiDAR DEM.

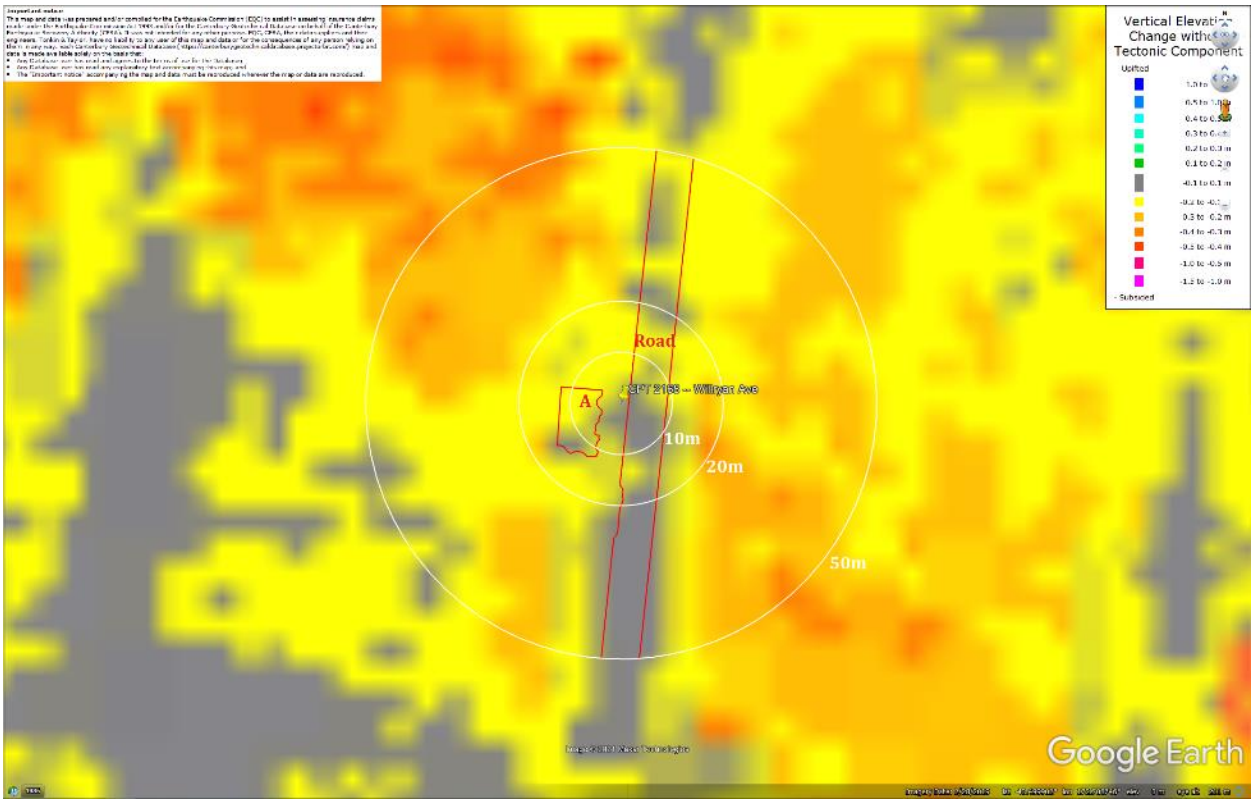

Figure 34: Ground surface subsidence without tectonic component for Feb 2011 Earthquake according to the LiDAR DEM.

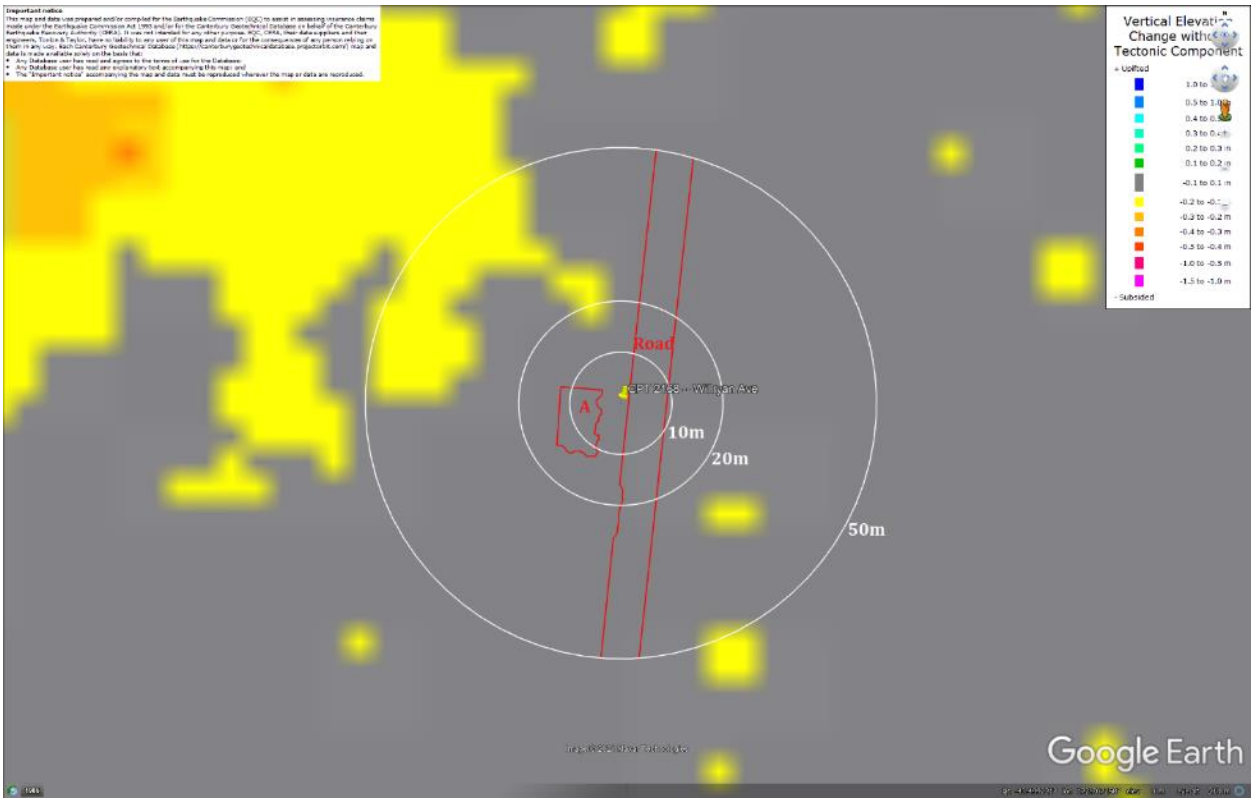

Figure 35: Ground surface subsidence without tectonic component for June 2011 Earthquake according to the LiDAR DEM.

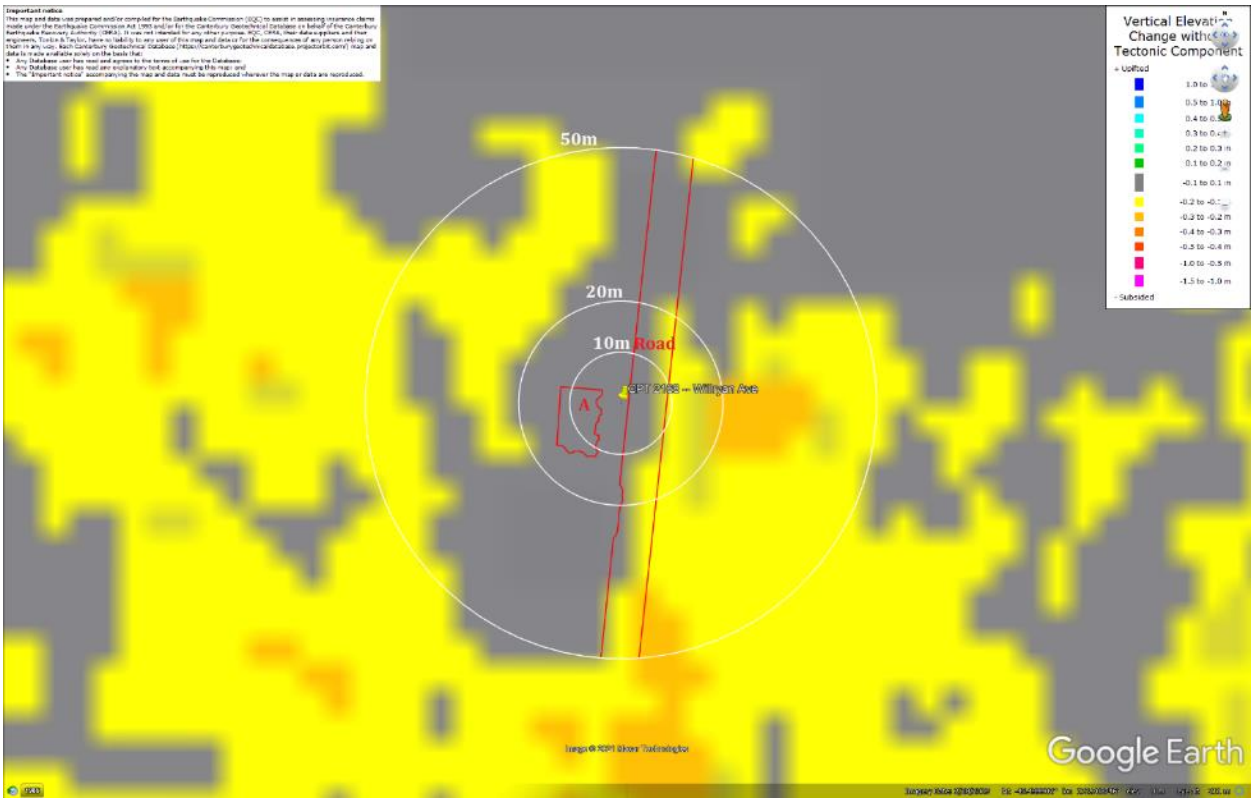

Figure 36: Ground surface subsidence without tectonic component for Dec 2011 Earthquake according to the LiDAR DEM.

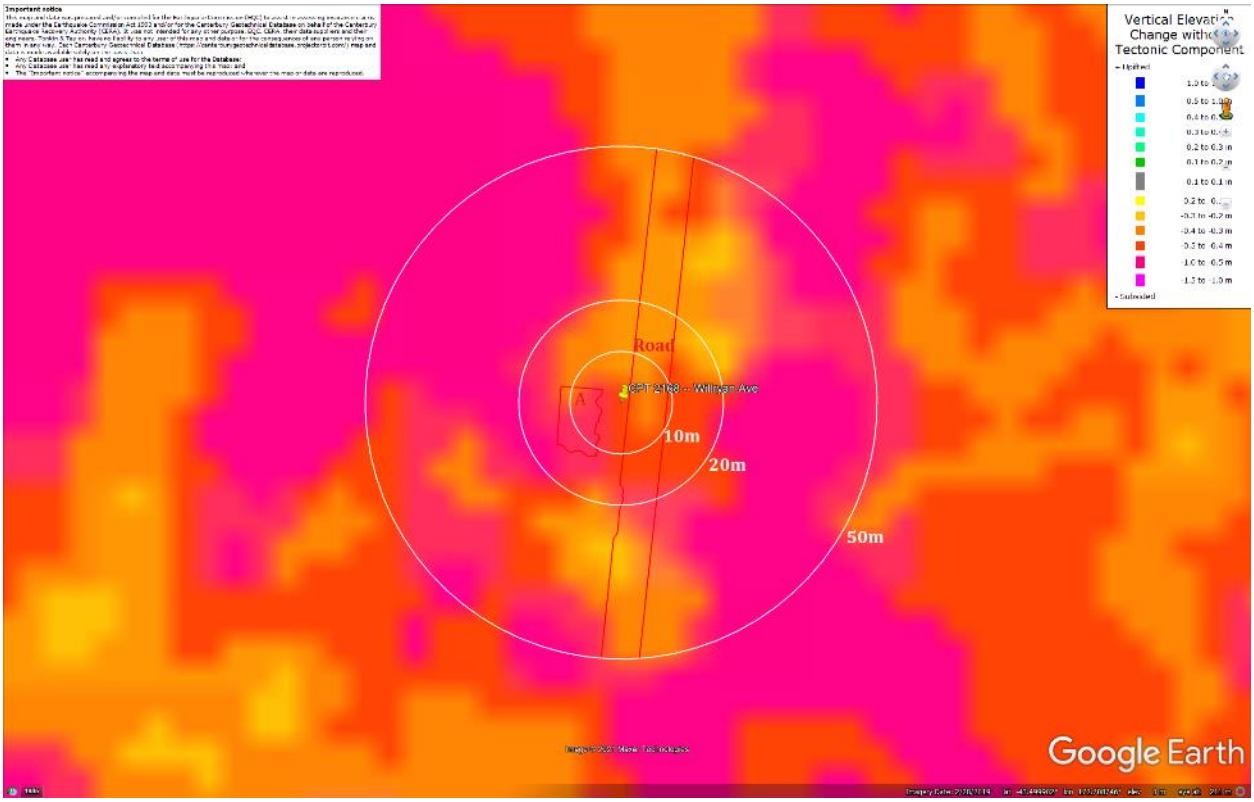

Figure 37: Ground surface subsidence without tectonic component for Canterbury Earthquake Sequence according to the LiDAR DEM.

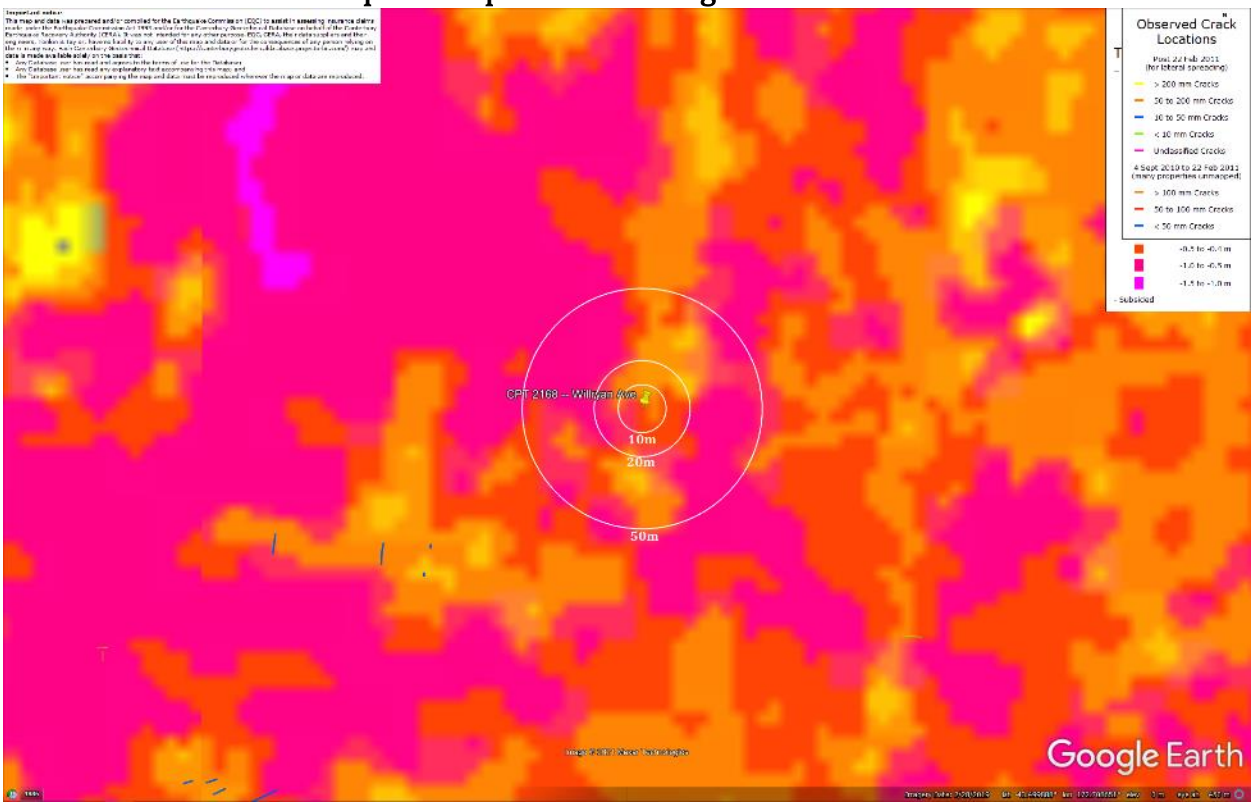

Figure 38: No lateral spreading for Canterbury Earthquake Sequence.

Figure 39: Vertical tectonic movements for Sep 2010 Earthquake.

Figure 40: Vertical tectonic movements for Feb 2011 Earthquake.

Figure 41: Vertical tectonic movements for June 2011 Earthquake.

Figure 42: Vertical tectonic movements for Dec 2011 Earthquake.

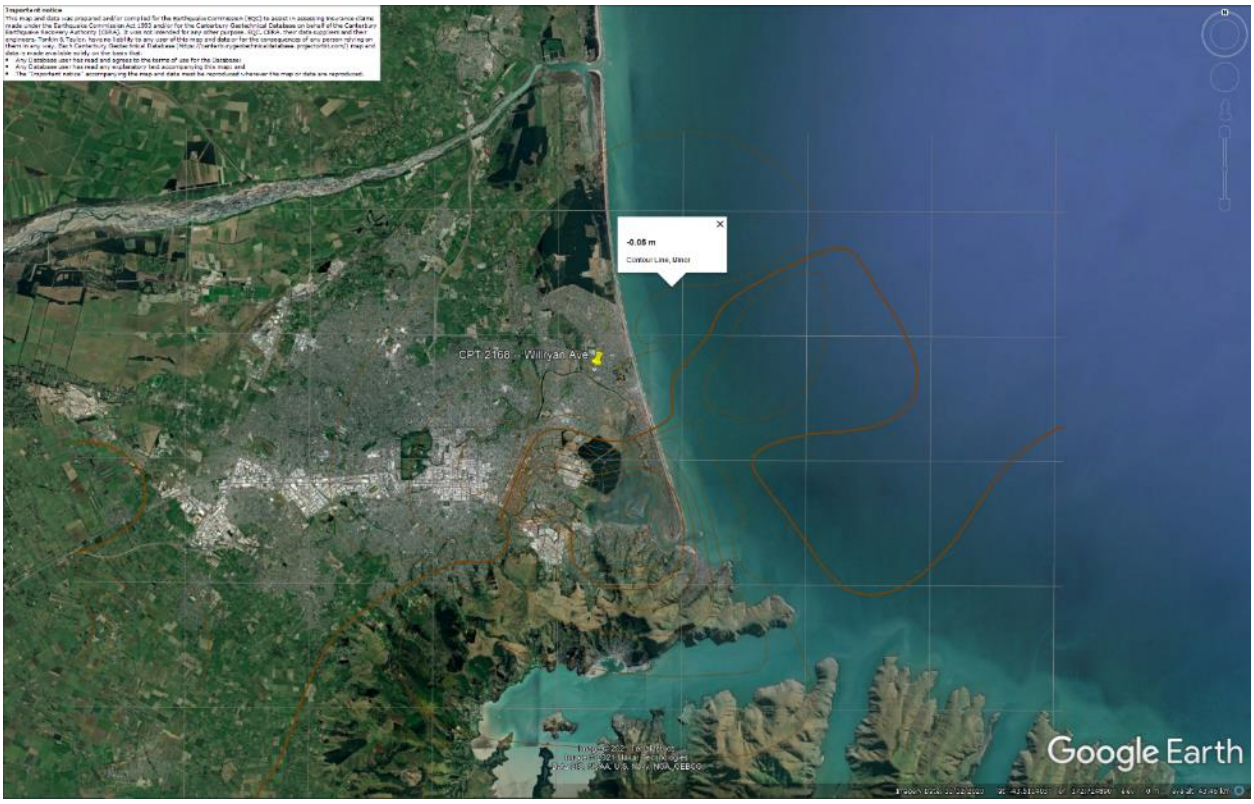

Figure 43: Vertical tectonic movements for Canterbury Earthquake Sequence.

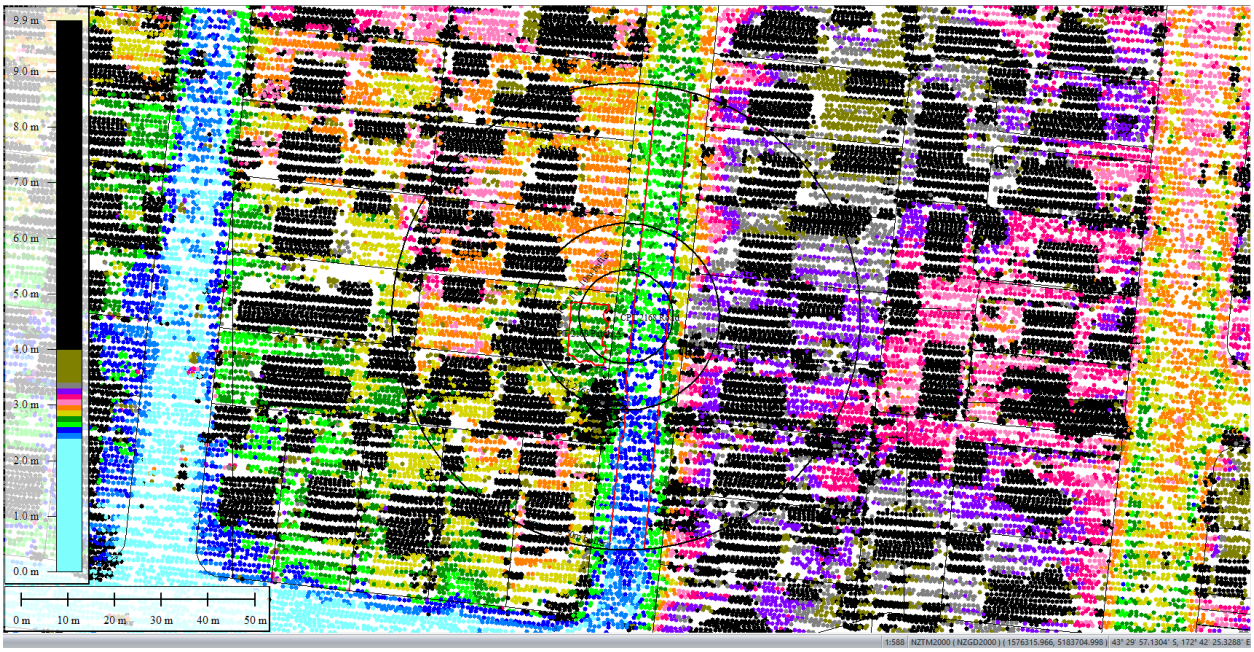

Figure 44: Sep 5, 2010 LiDAR survey.

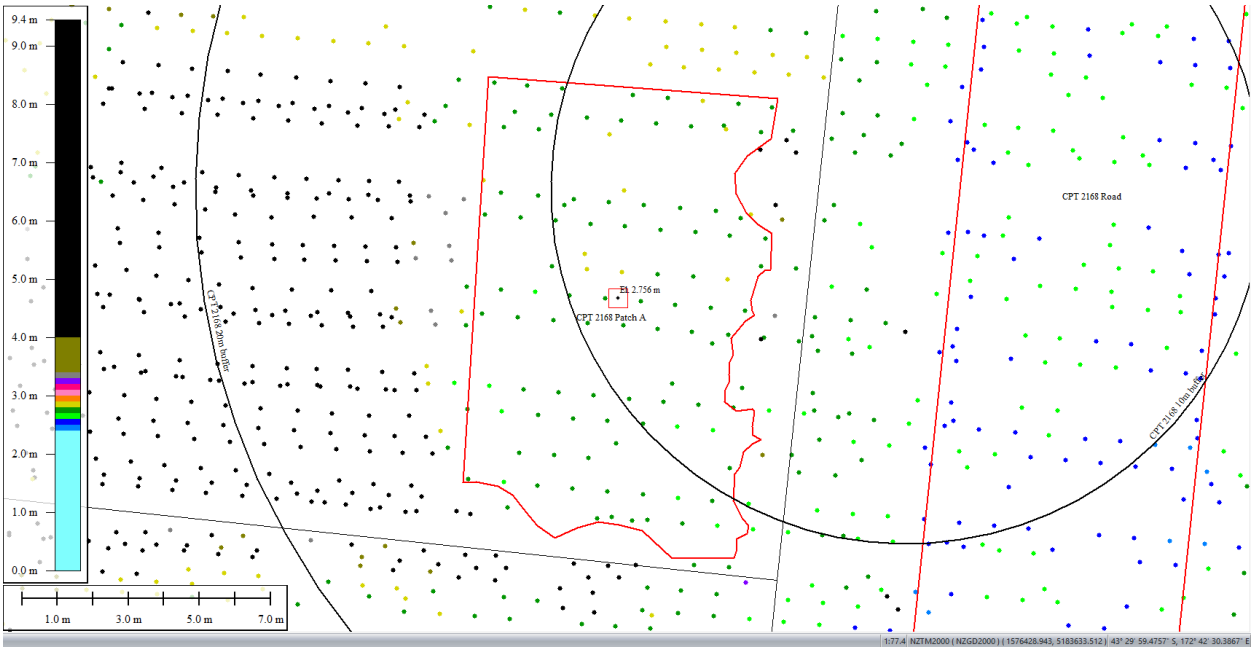

Figure 45: Ground surface elevation averaged over 10-m, 20-m, and 50-m buffers for Patch A for Sep 5, 2010 LiDAR survey.

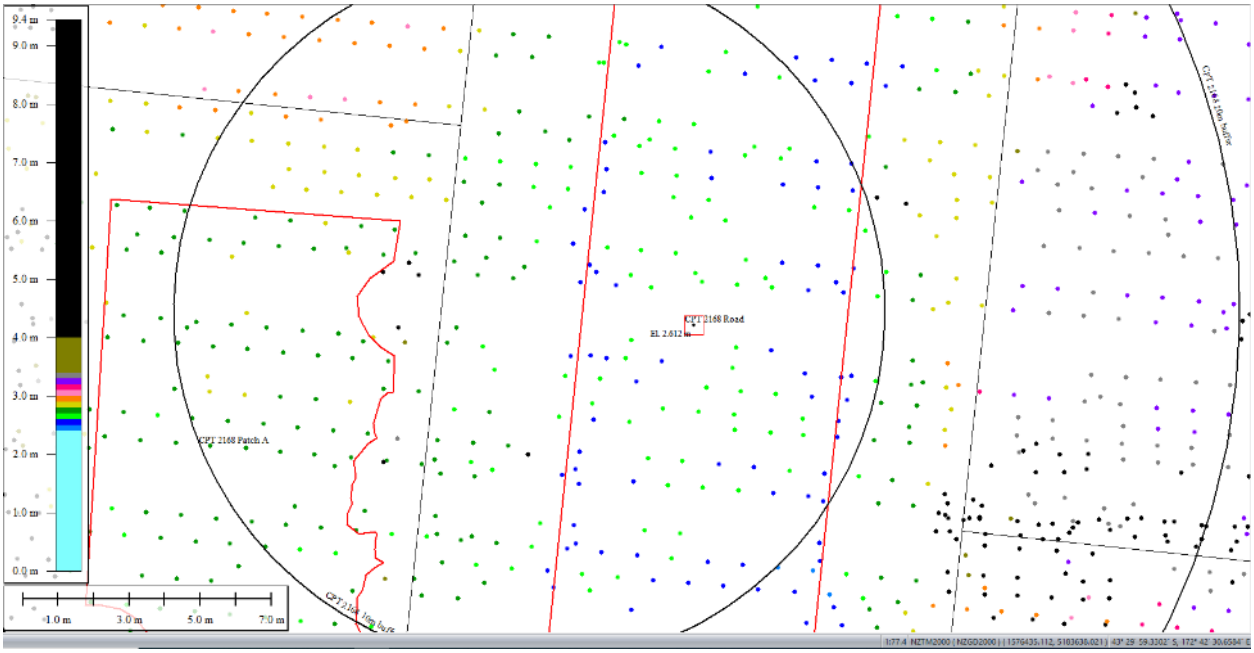

Figure 46: Ground surface elevation averaged over 10-m buffer for Road for Sep 5, 2010 LiDAR survey.

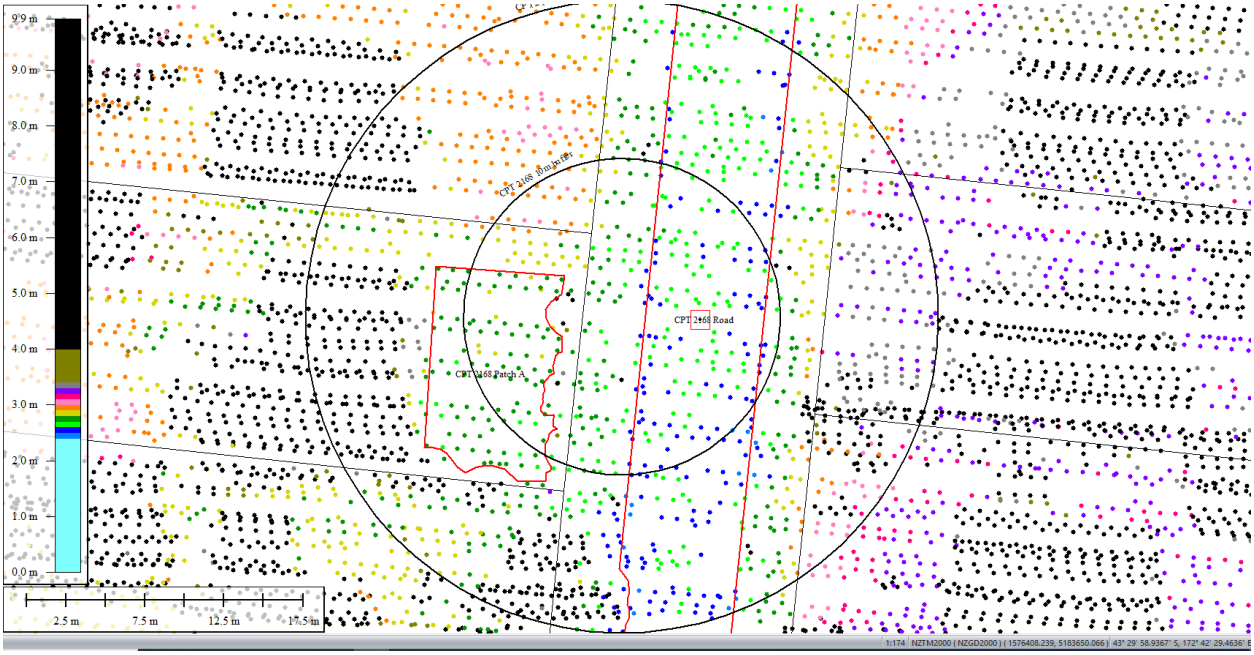

Figure 47: Ground surface elevation averaged over 20-m buffer for Road for Sep 5, 2010 LiDAR survey (el. 2.498m).

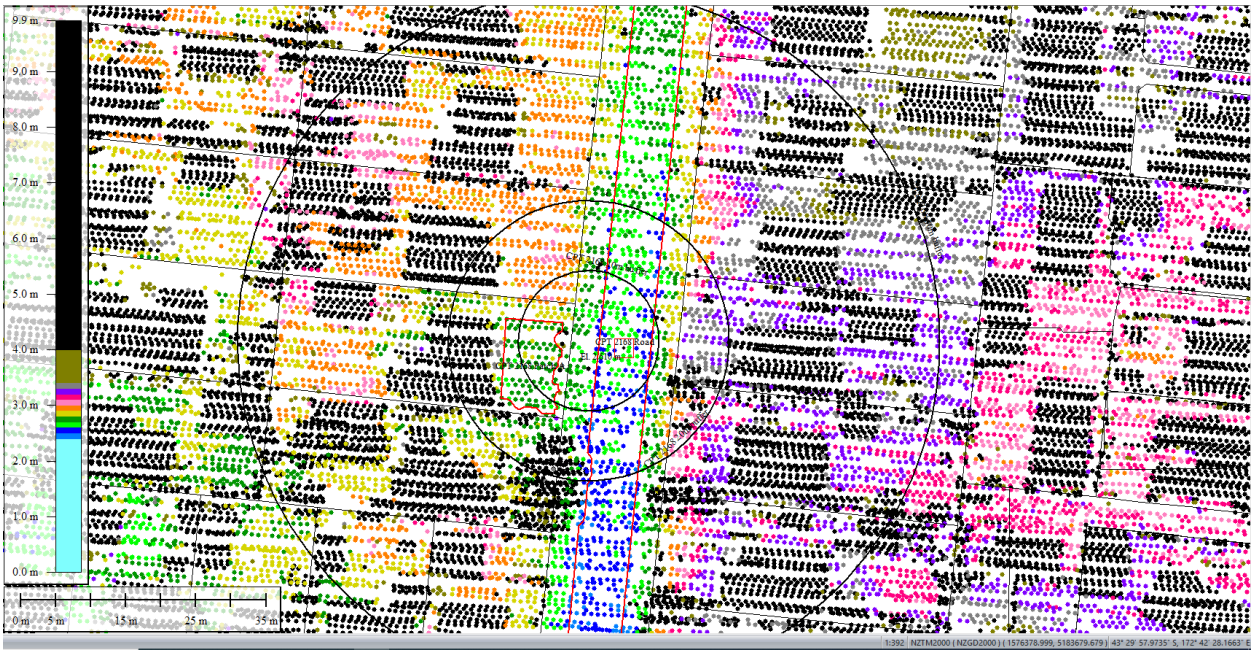

Figure 48: Ground surface elevation averaged over 50-m buffer for Road for Sep 5, 2010 LiDAR survey.

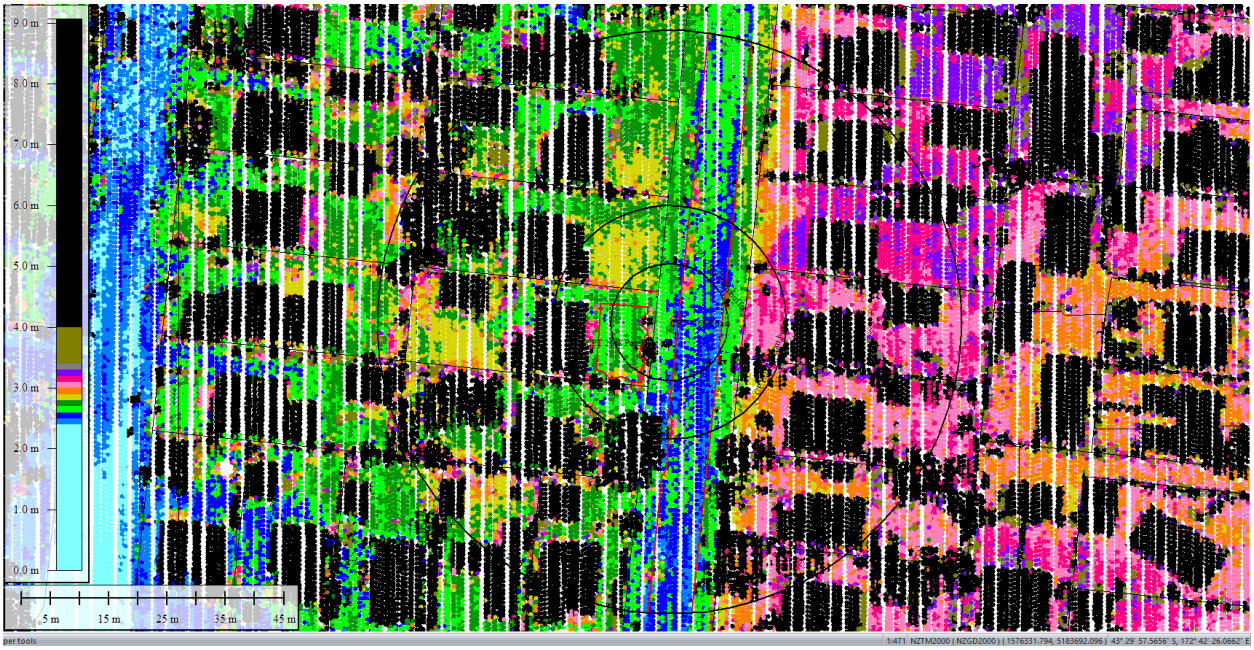

Figure 49: Mar 2011 LiDAR survey.

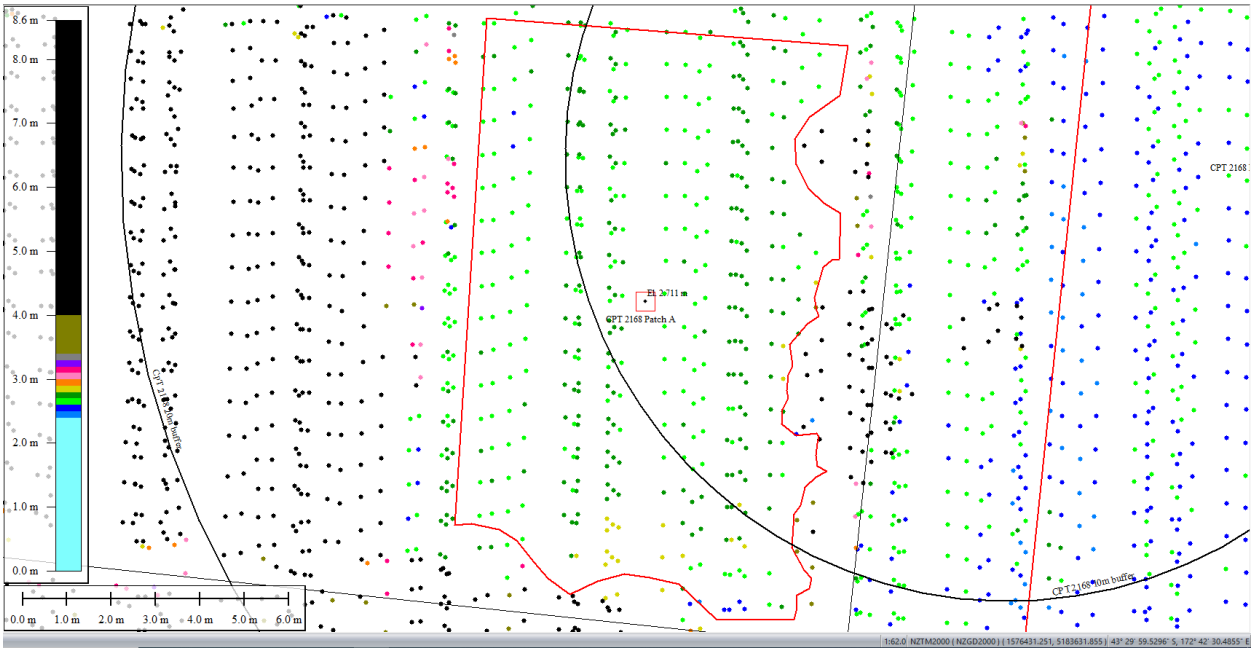

Figure 50: Ground surface elevation averaged over 10-m, 20-m, and 50-m buffers for Patch A for Mar 2011 LiDAR survey.

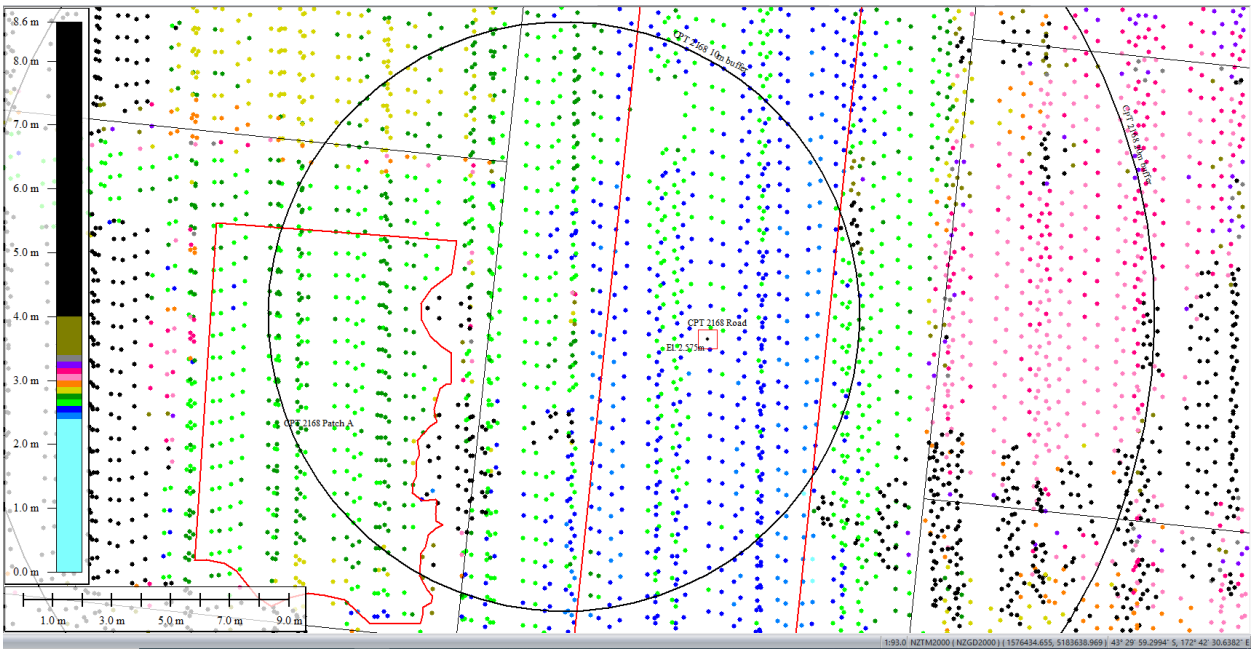

Figure 51: Ground surface elevation averaged over 10-m buffer for Road for Mar 2011 LiDAR survey.

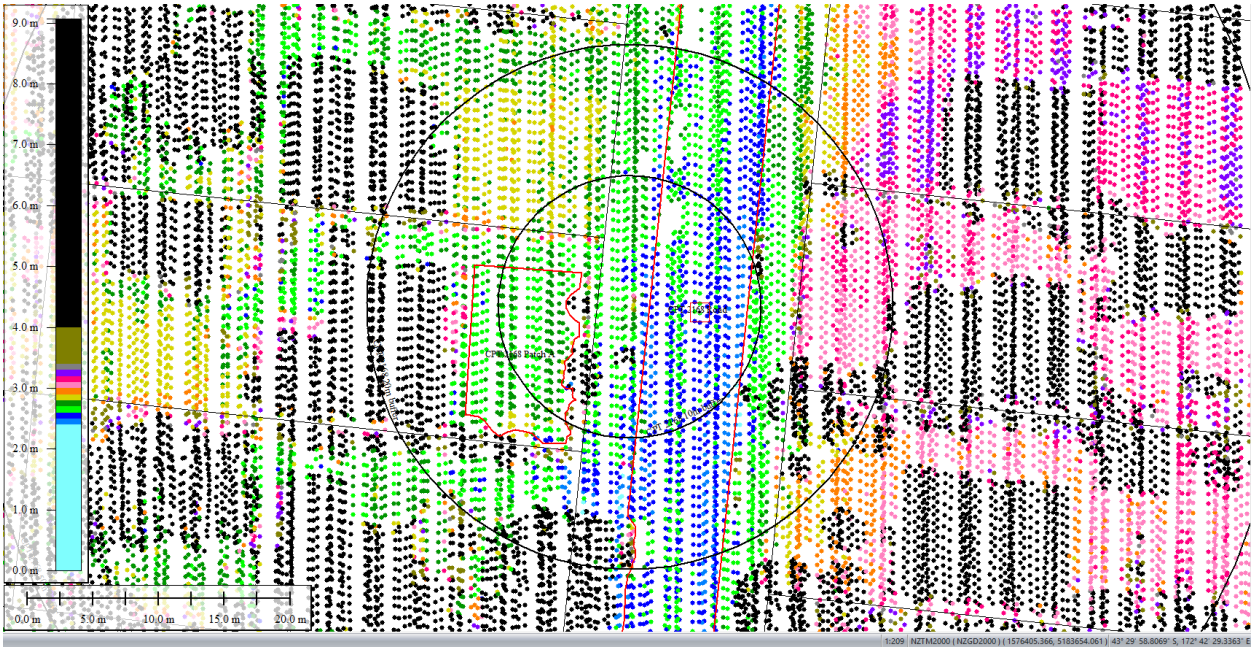

Figure 52: Ground surface elevation averaged over 20-m buffer for Road for Mar 2011 LiDAR survey.

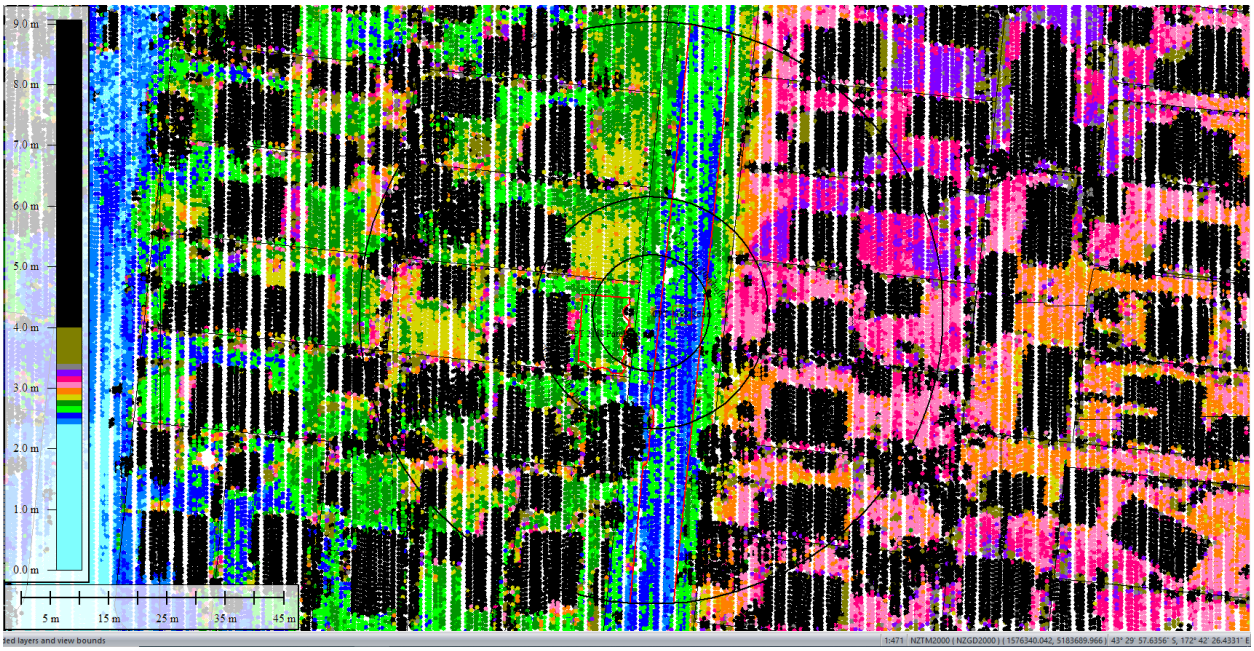

Figure 53: Ground surface elevation averaged over 50-m buffer for Road for Mar 2011 LiDAR survey.

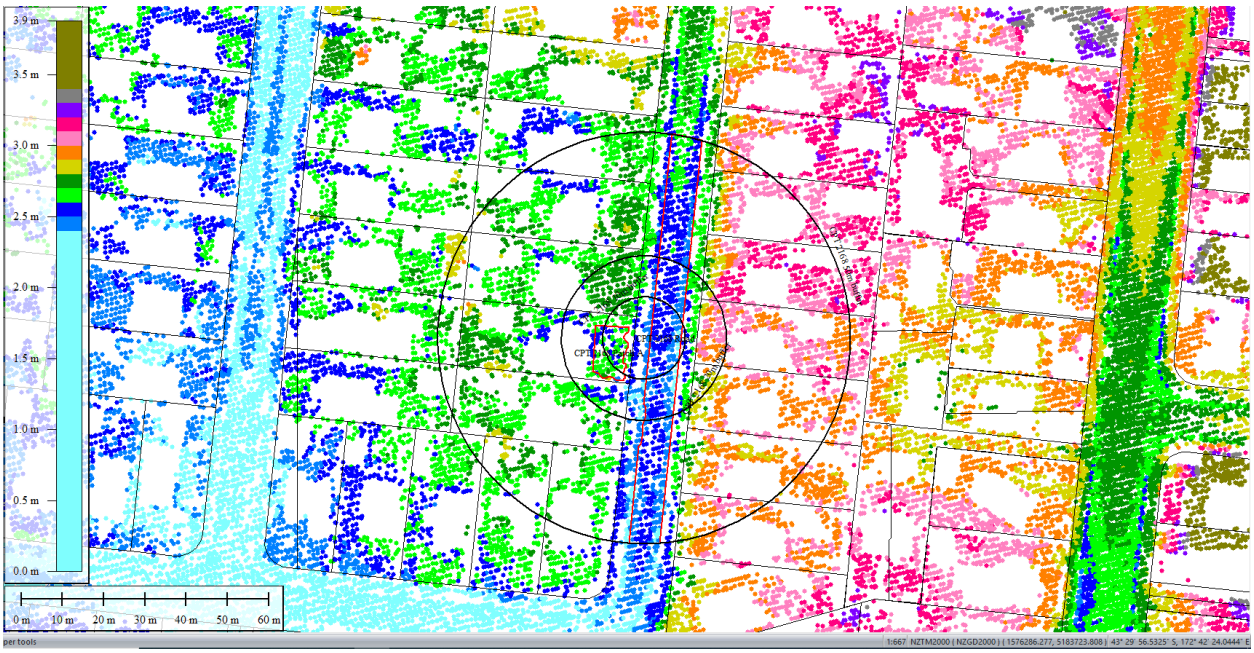

Figure 54: May 2011 LiDAR survey.

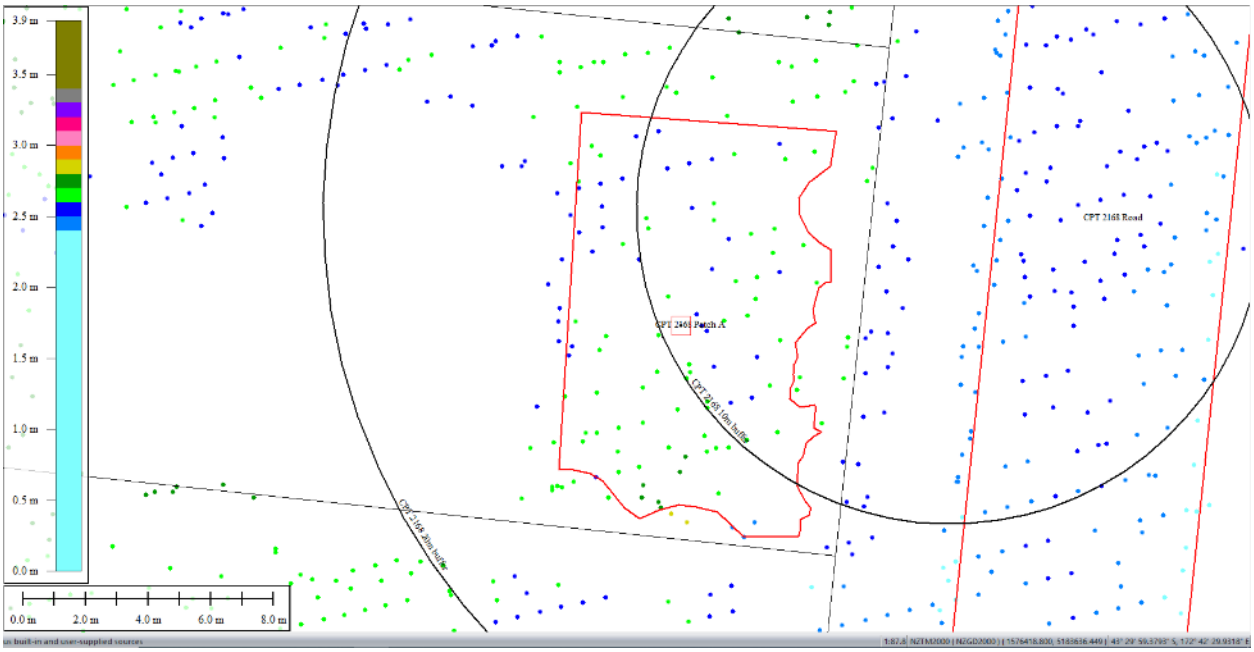

Figure 55: Ground surface elevation averaged over 10-m, 20-m, and 50-m buffers for Patch A for May 2011 LiDAR survey (el. 2.624m).

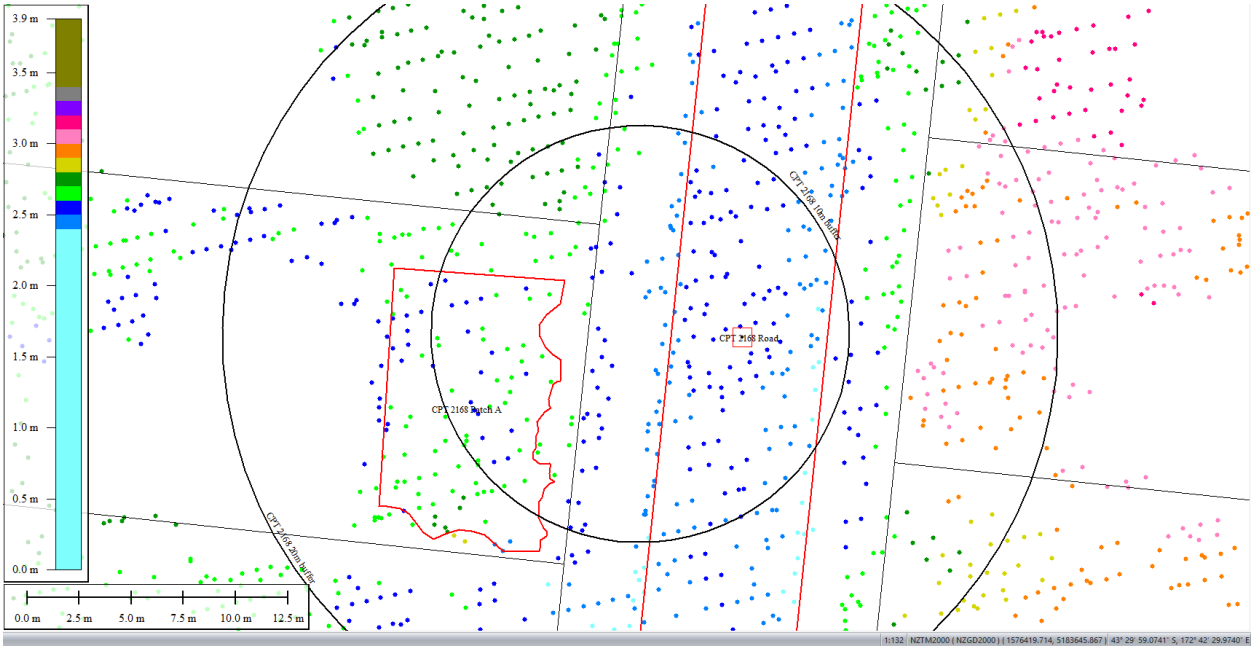

Figure 56: Ground surface elevation averaged over 10-m buffer for Road for May 2011 LiDAR survey (el. 2.498m).

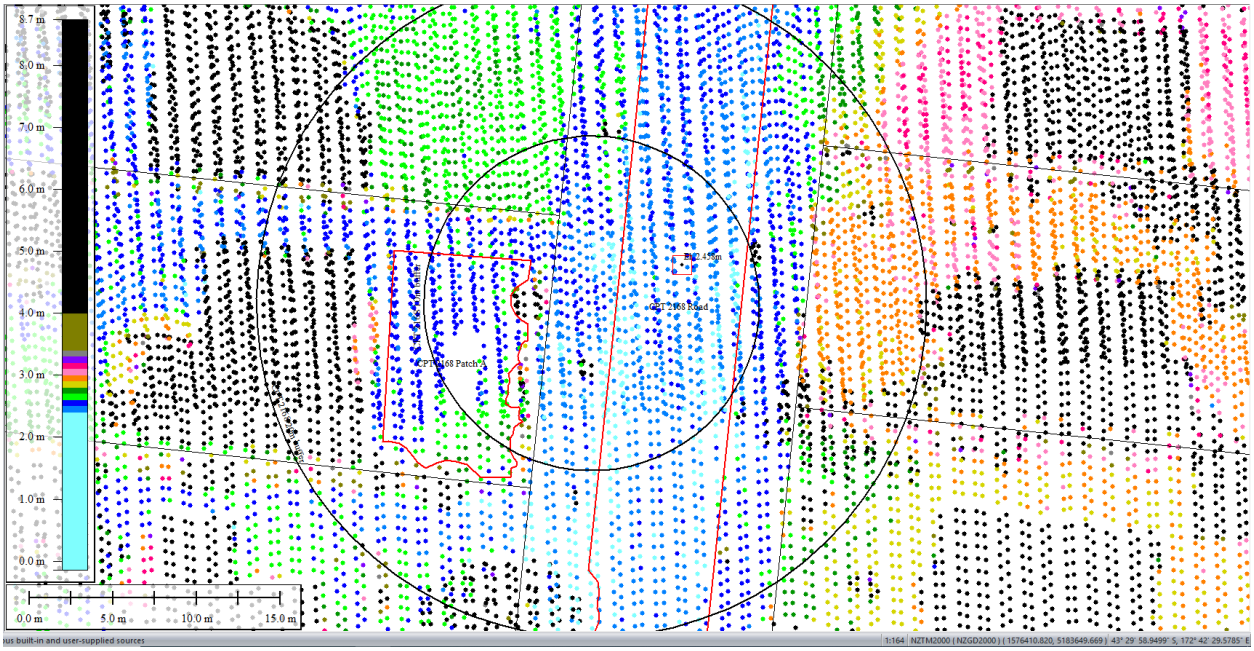

Figure 57: Ground surface elevation averaged over 20-m buffer for Road for May 2011 LiDAR survey.

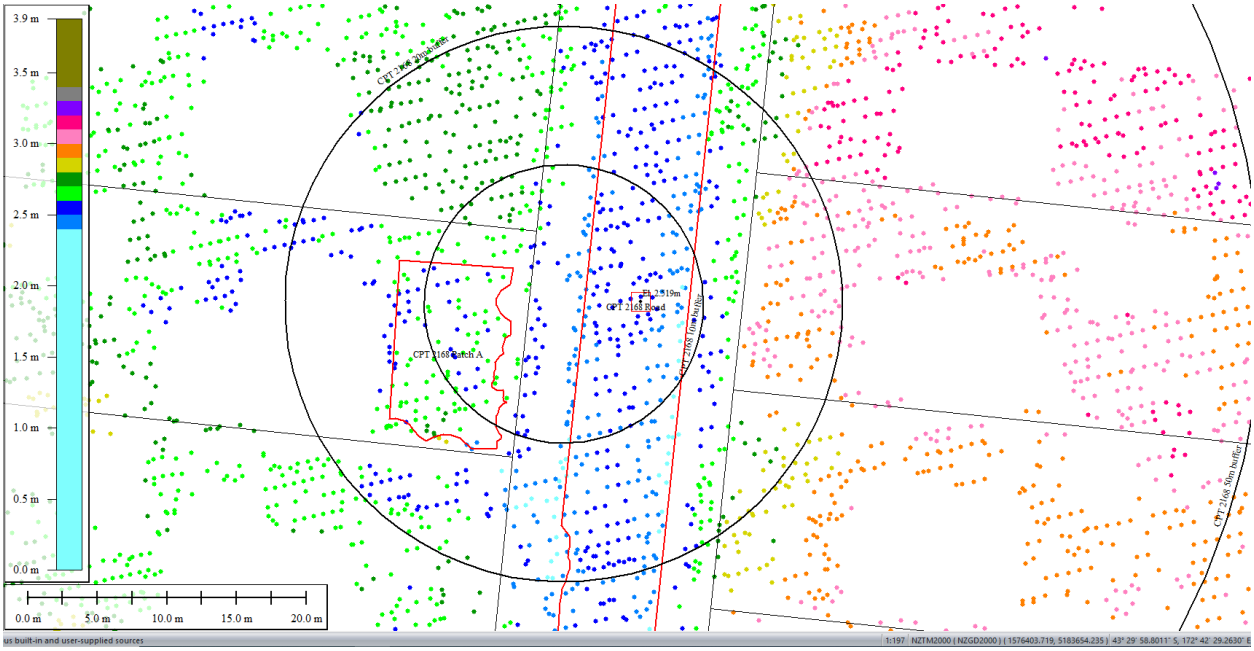

Figure 58: Ground surface elevation averaged over 50-m buffer for Road for May 2011 LiDAR survey.

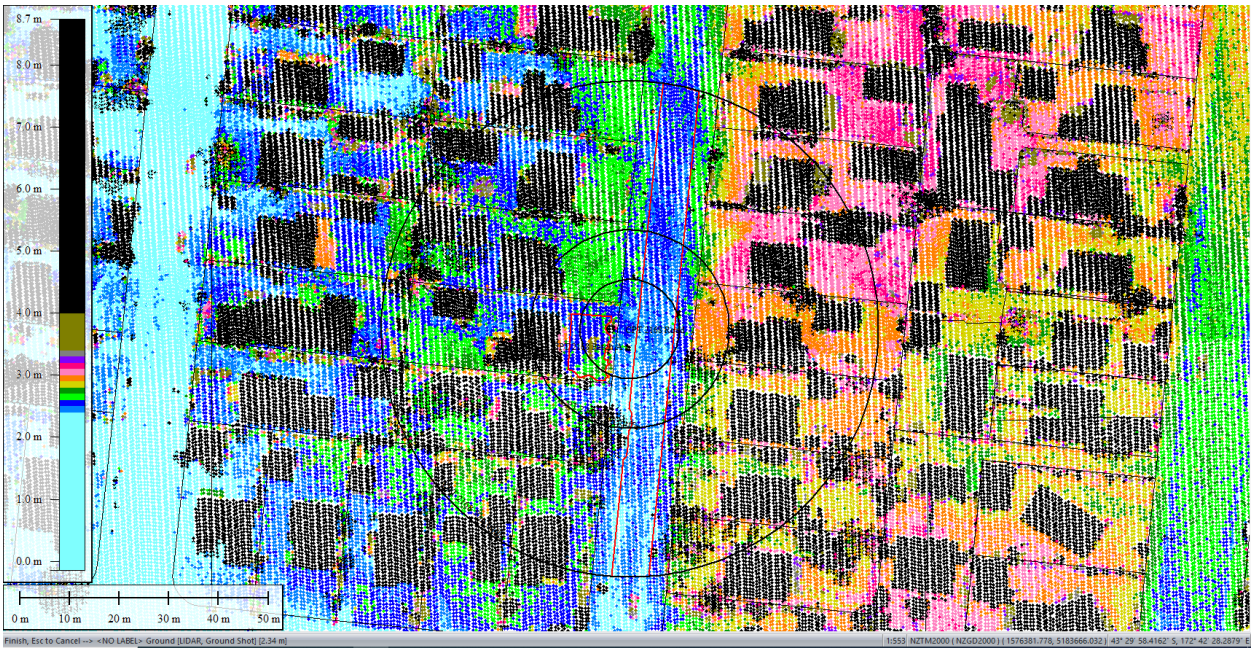

Figure 59: Sep 2011 LiDAR survey.

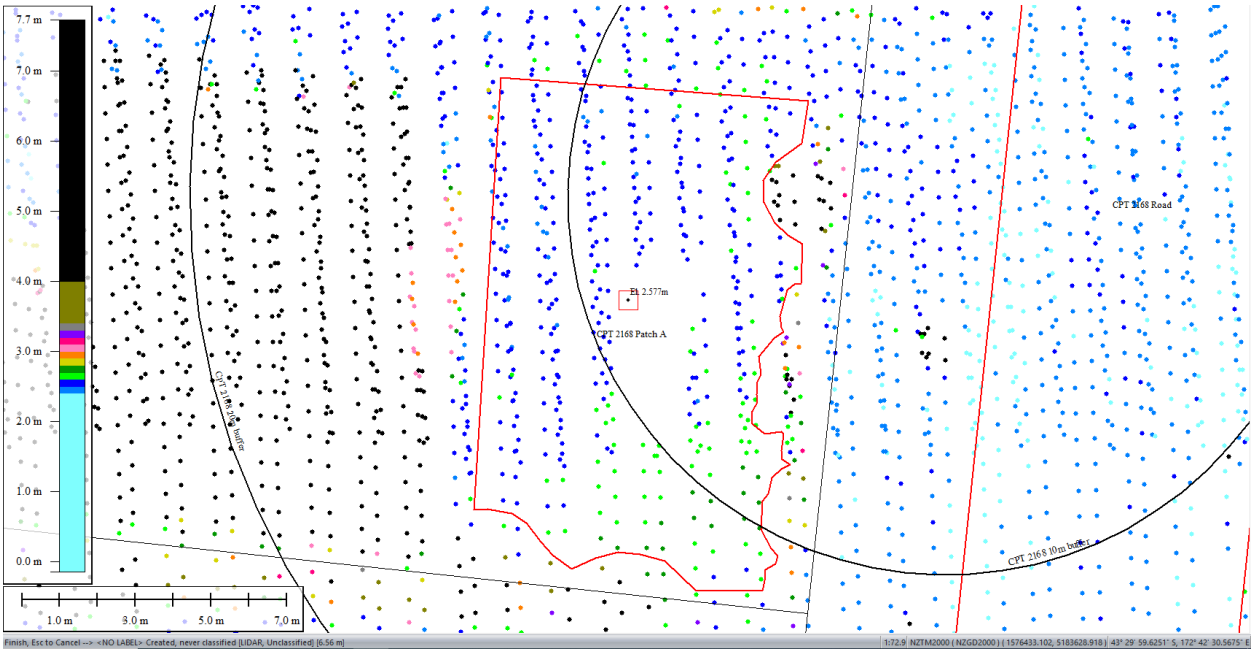

Figure 60: Ground surface elevation averaged over 10-m, 20-m, and 50-m buffers for Patch A for Sep 2011 LiDAR survey.

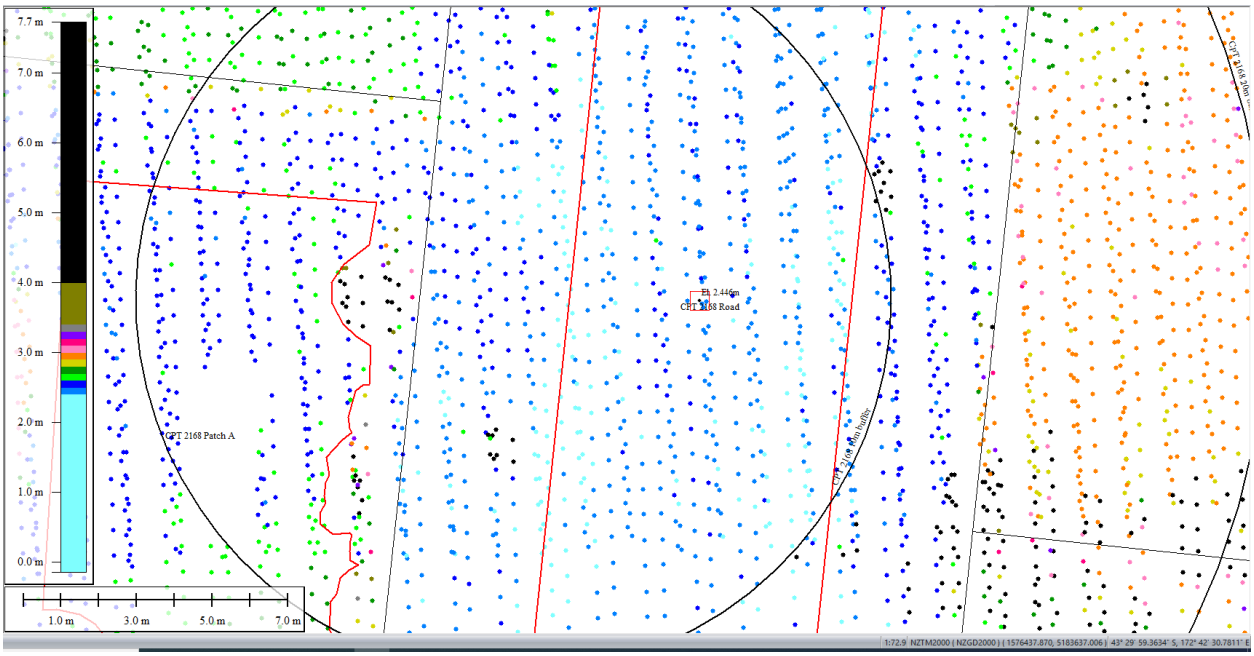

Figure 61: Ground surface elevation averaged over 10-m buffer for Road for Sep 2011 LiDAR survey.

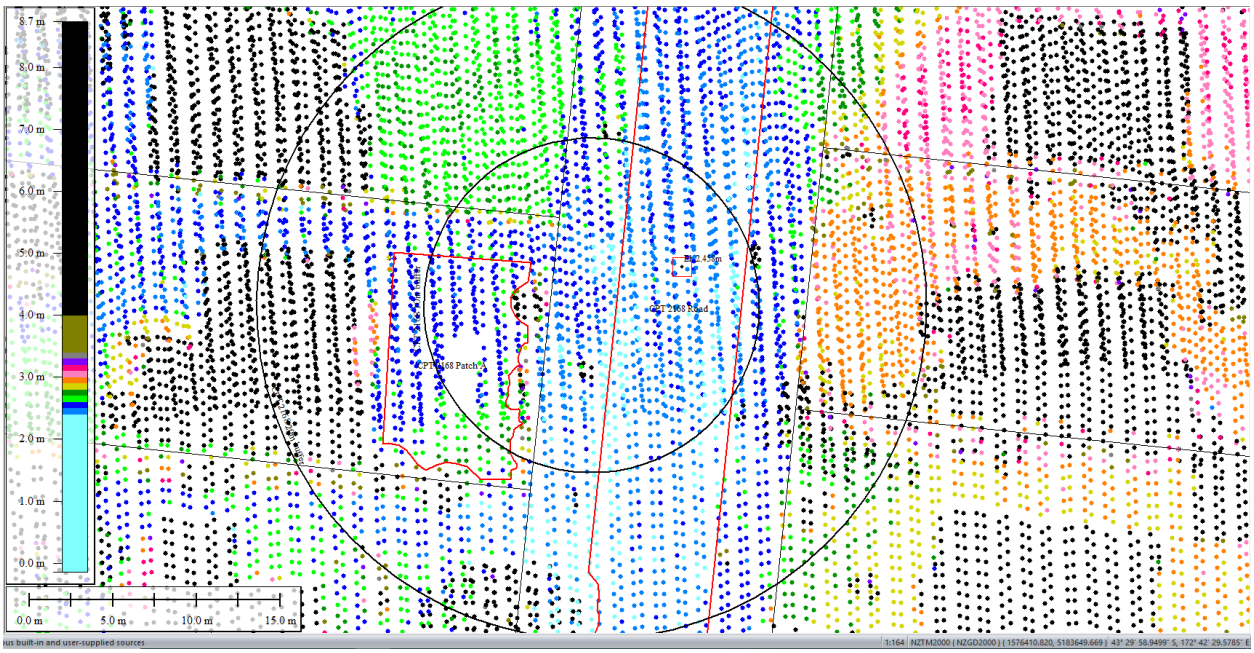

Figure 62: Ground surface elevation averaged over 20-m buffer for Road for Sep 2011 LiDAR survey.

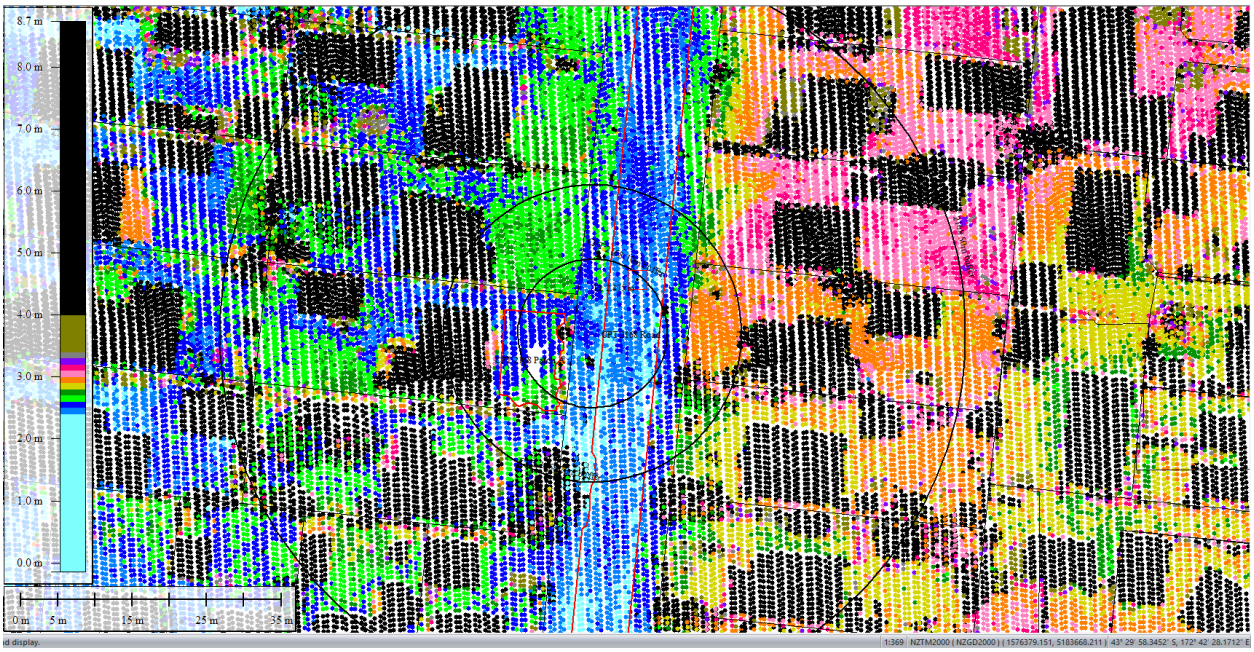

Figure 63: Ground surface elevation averaged over 50-m buffer for Road for Sep 2011 LiDAR survey.

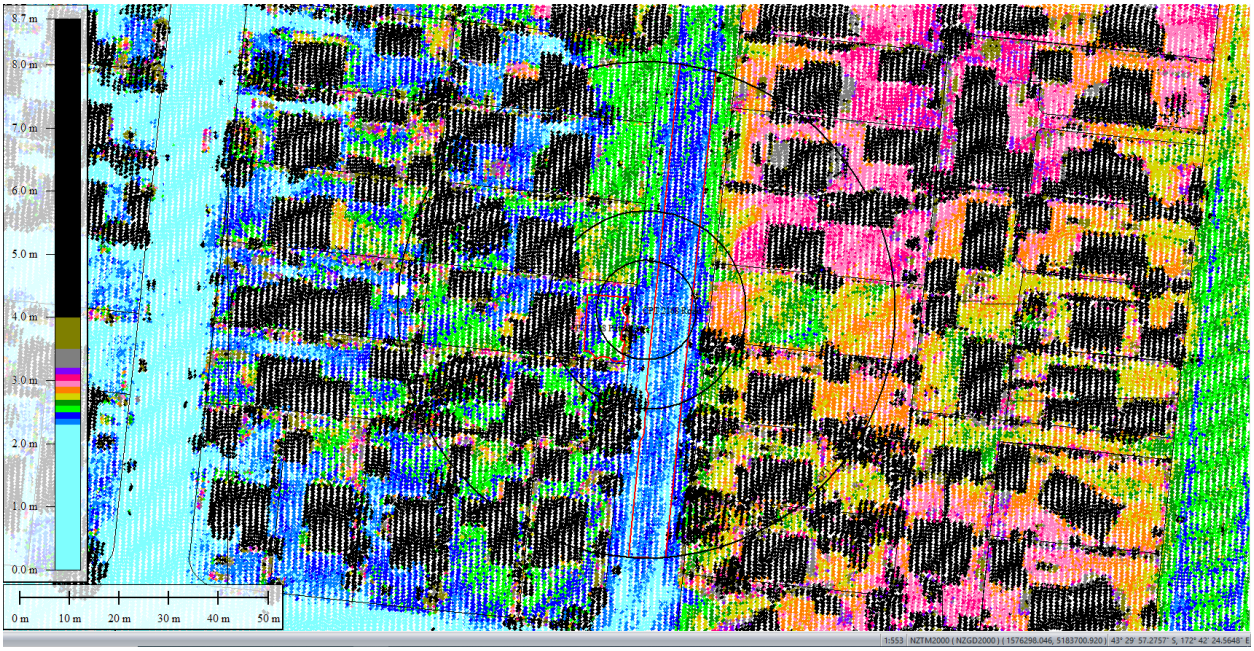

Figure 64: Feb 2012 LiDAR survey.

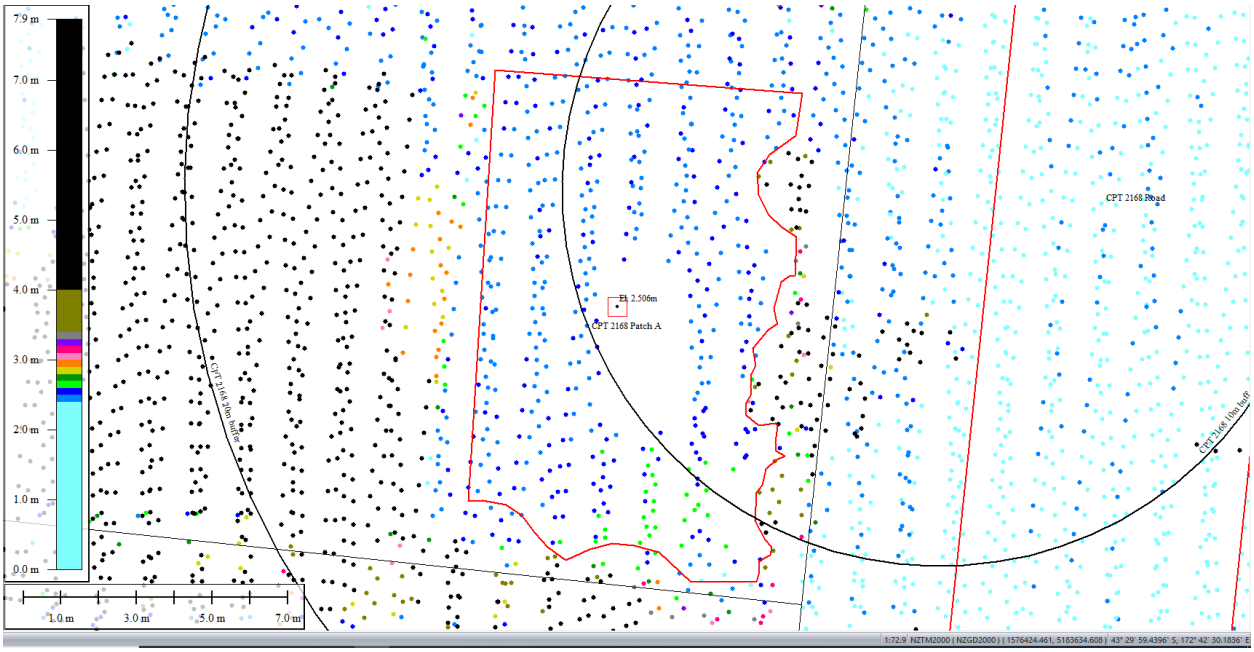

Figure 65: Ground surface elevation averaged over 10-m, 20-m, and 50-m buffers for Patch A for Feb 2012 LiDAR survey.

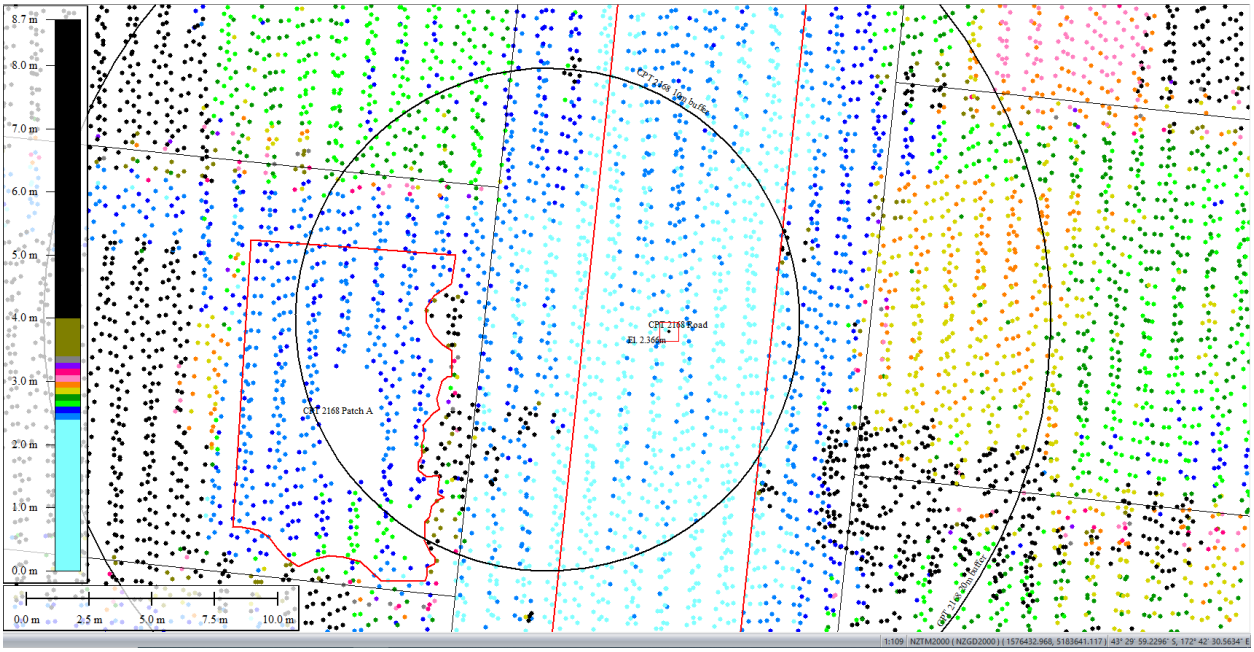

Figure 66: Ground surface elevation averaged over 10-m buffer for Road for Feb 2012 LiDAR survey.

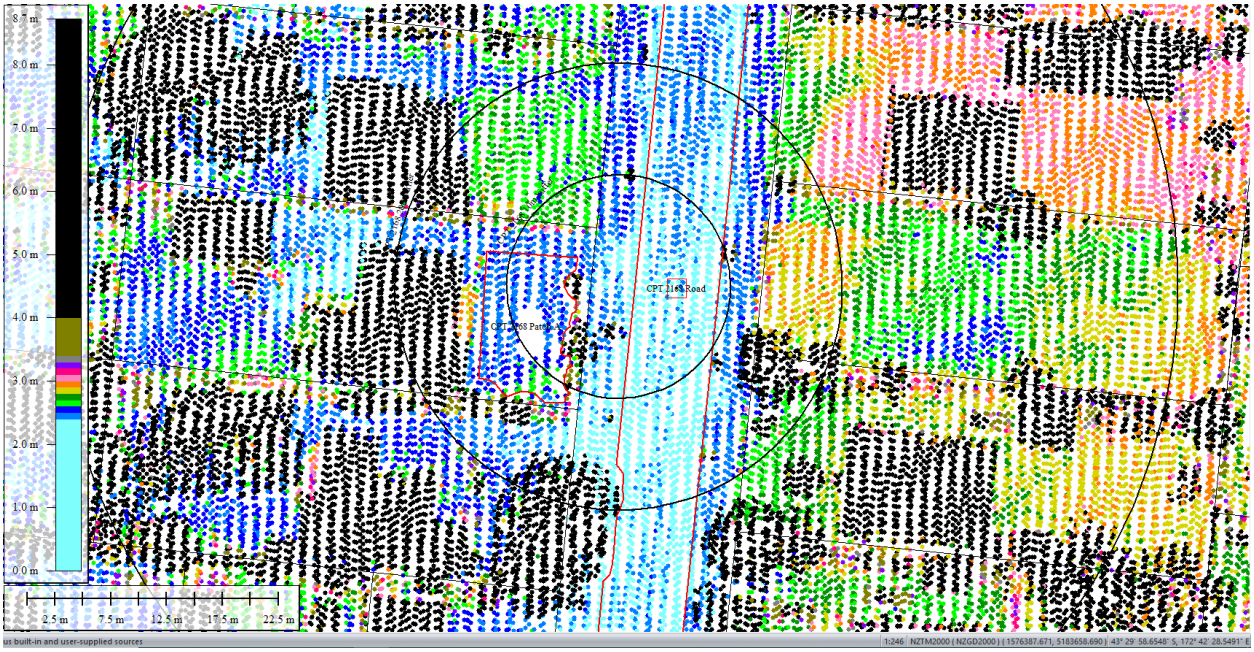

Figure 67: Ground surface elevation averaged over 20-m buffer for Road for Feb 2012 LiDAR survey (el. 2.370m).

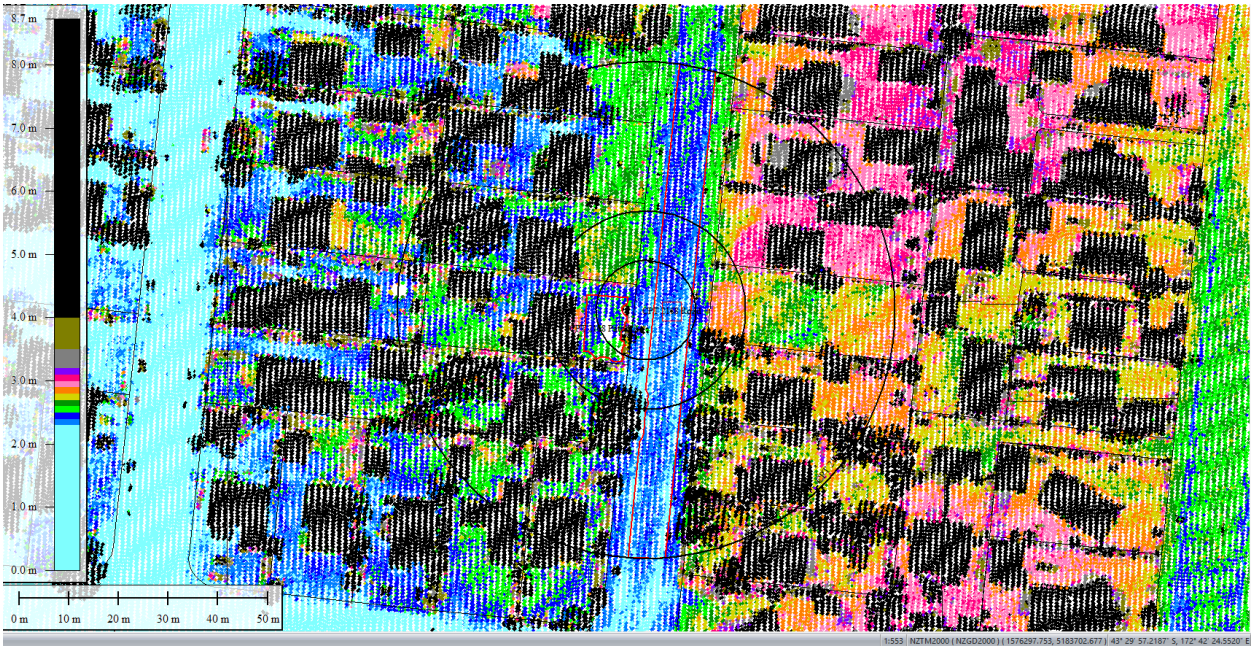

Figure 68: Ground surface elevation averaged over 50-m buffer for Road for Feb 2012 LiDAR survey (el. 2.388m).

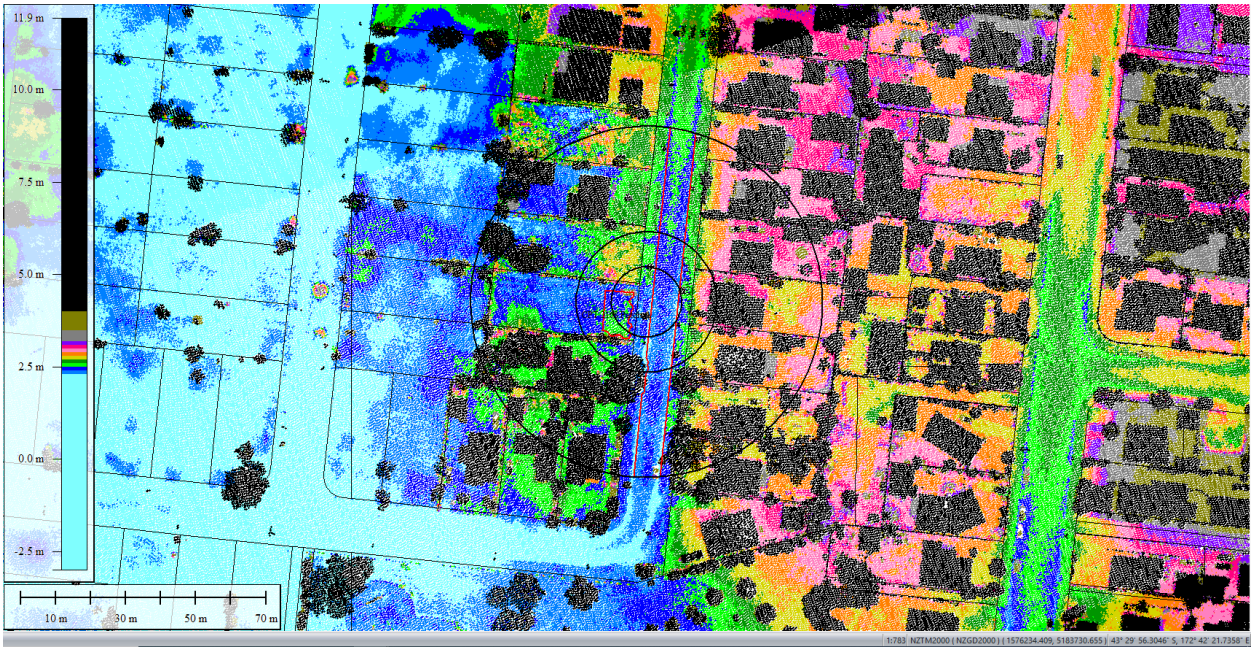

Figure 69: Oct 2015 LiDAR survey.

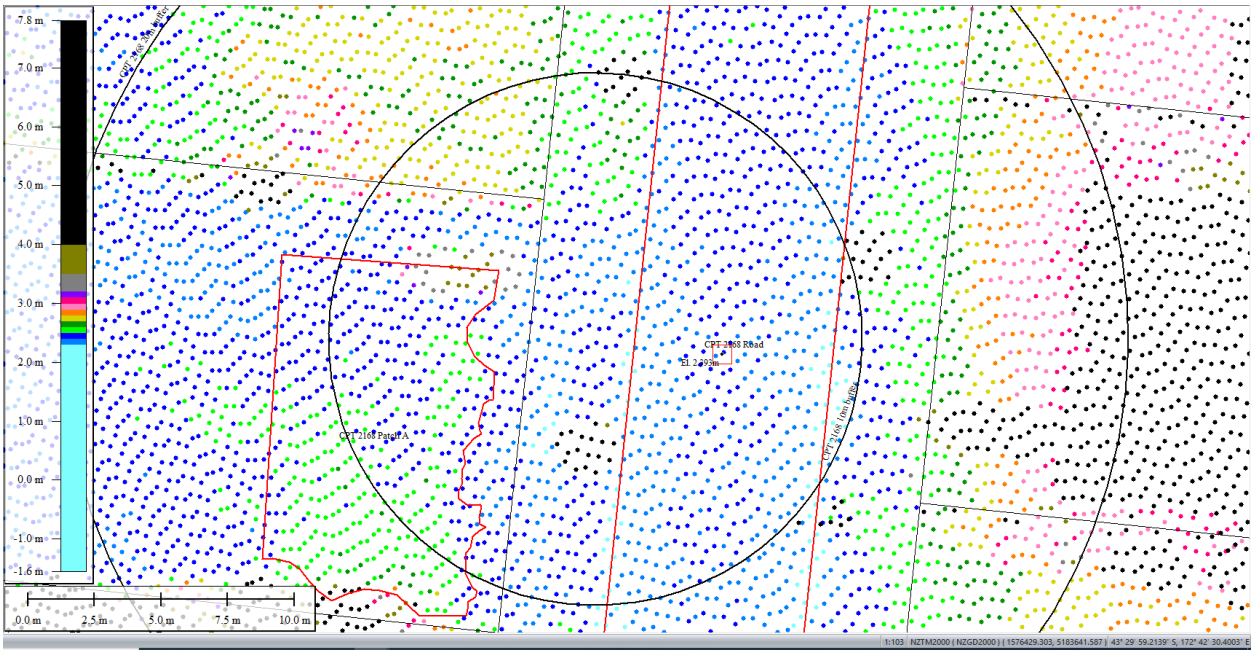

Figure 70: Ground surface elevation averaged over 10-m buffer for Road for Oct 2015 LiDAR survey.

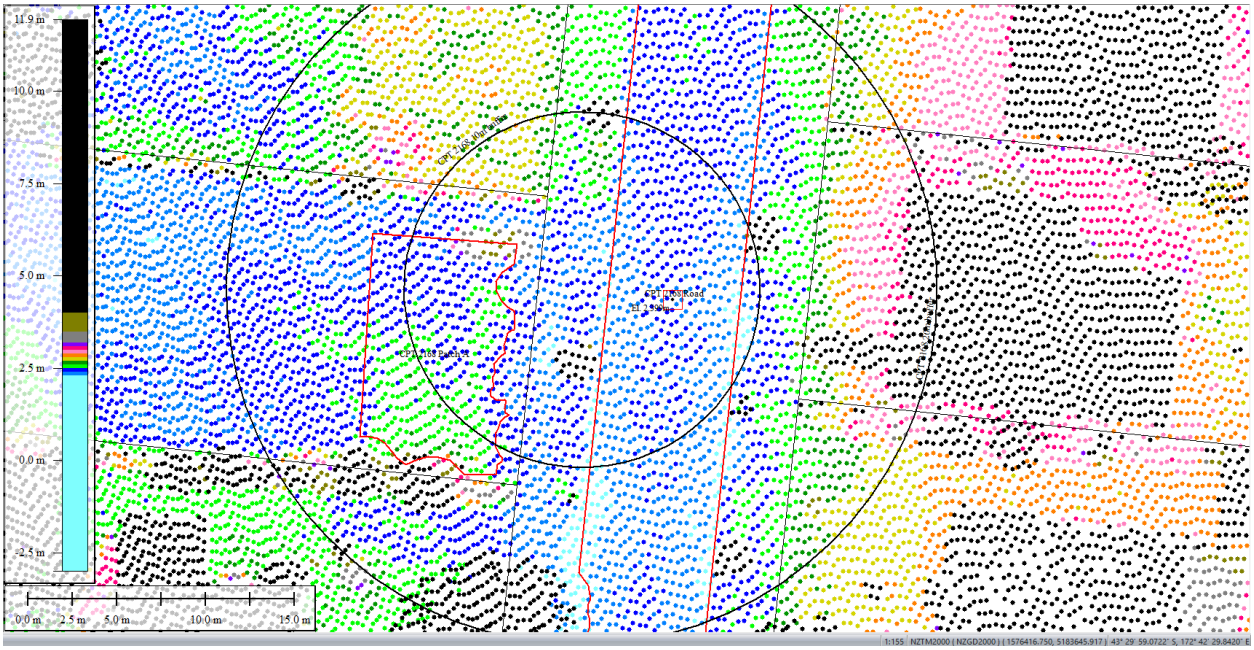

Figure 71: Ground surface elevation averaged over 20-m buffer for Road for Oct 2015 LiDAR survey.

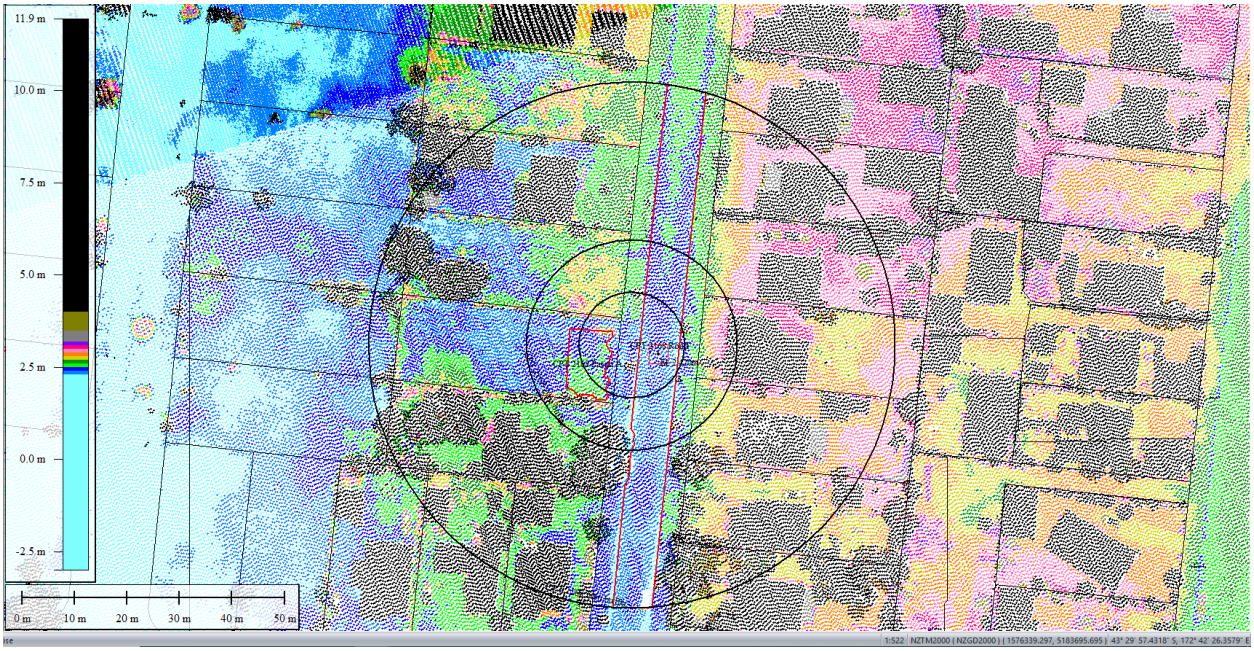

Figure 72: Ground surface elevation averaged over 50-m buffer for Road for Oct 2015 LiDAR survey.

Figure 73: Aerial photograph showing the ejecta outline at the site for Feb-11 EQ.

Figure 74: Aerial photograph acquired on 16 Jun 2011 showing the ejecta outline at the site for Jun-11 EQ.

Figure 75: Aerial photograph showing the ejecta outline at the site for Dec-11 EQ.

Contents of this figure cannot be shared as doing so is restricted by a Non-Disclosure Agreement.

Figure 76: LDAT inspection notes for the property with Patch A (inspection date: 2 June 2011).

Figure 77: Ground photographs showing the undulating land and the sinkhole at the property with Patch A (photograph date: 2 June 2011).

Figure 78: Ground photographs showing ejecta remnants at properties within the 50-m buffer showing (photograph date: 2 June 2011).

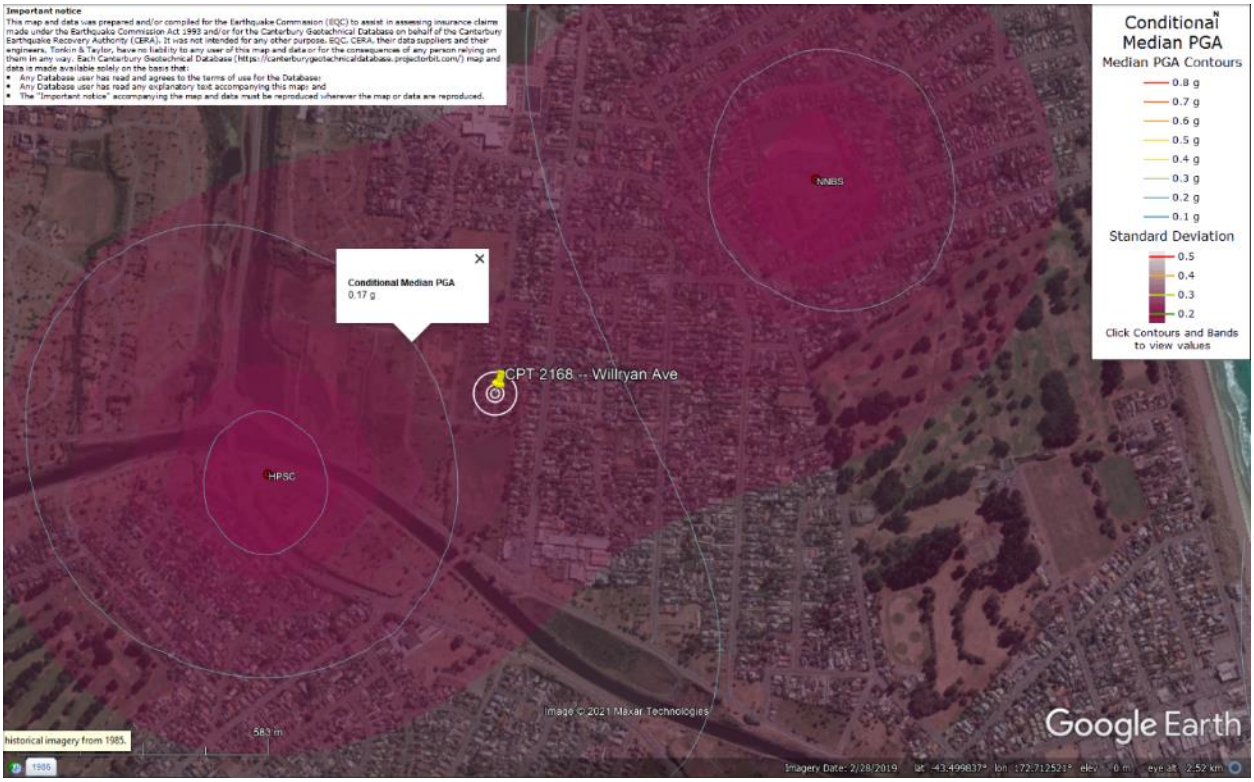

Figure 79: PGA for Sep-10 EQ (st. dev. = 0.225-0.250 ln units).

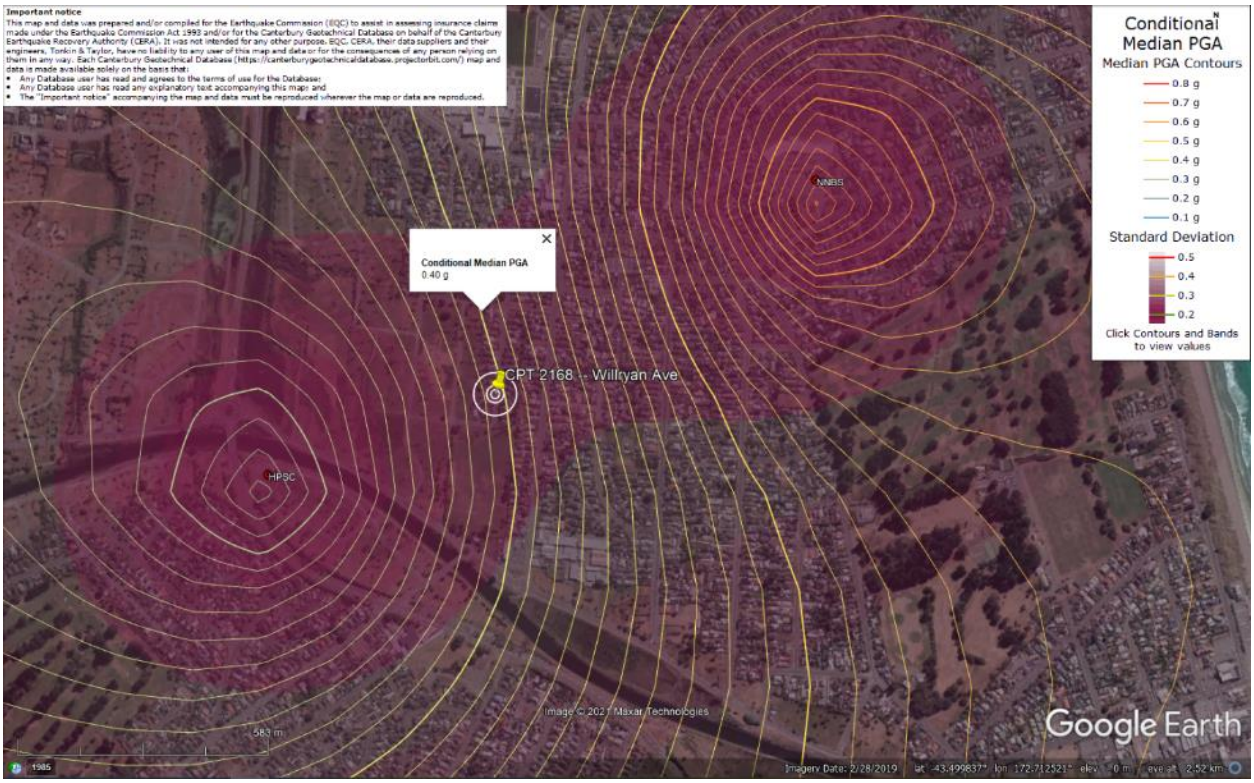

Figure 80: PGA for Feb-11 EQ (st. dev. = 0.250-0.275 ln units).

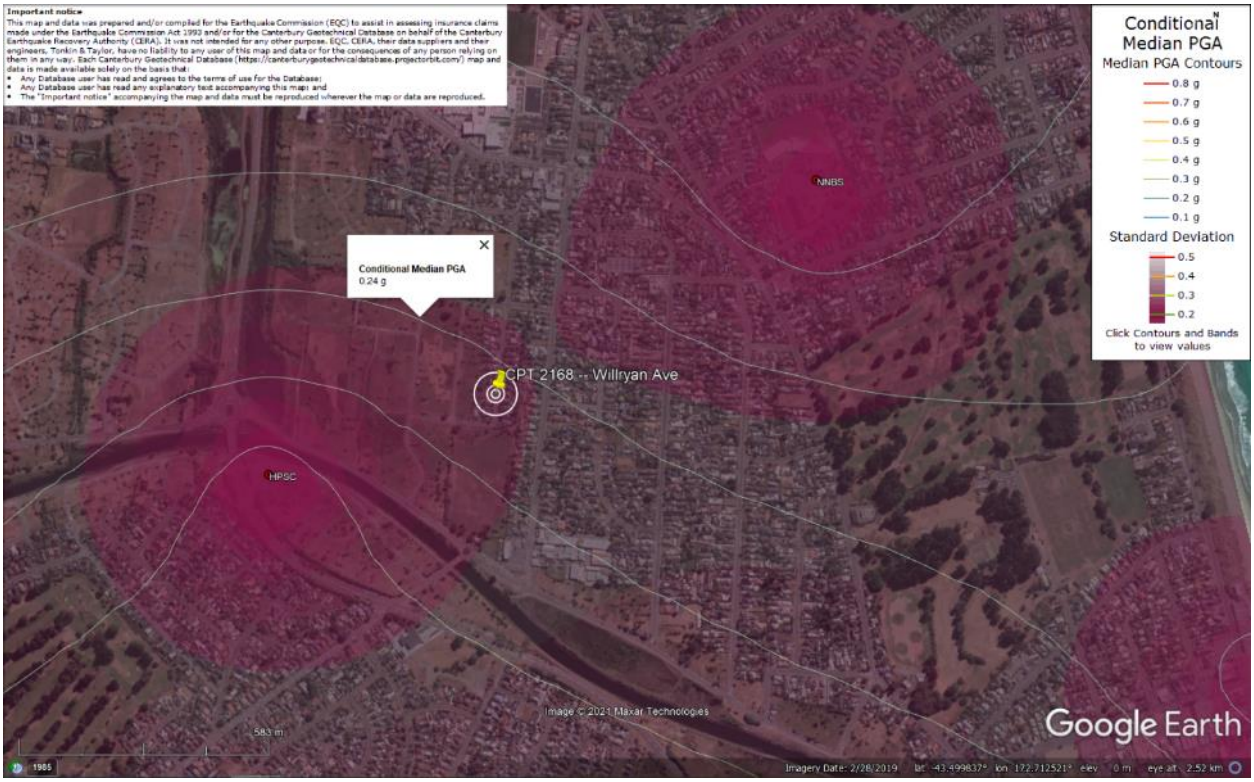

Figure 81: PGA for Jun-11 EQ (st. dev. = 0.250-0.275 ln units).

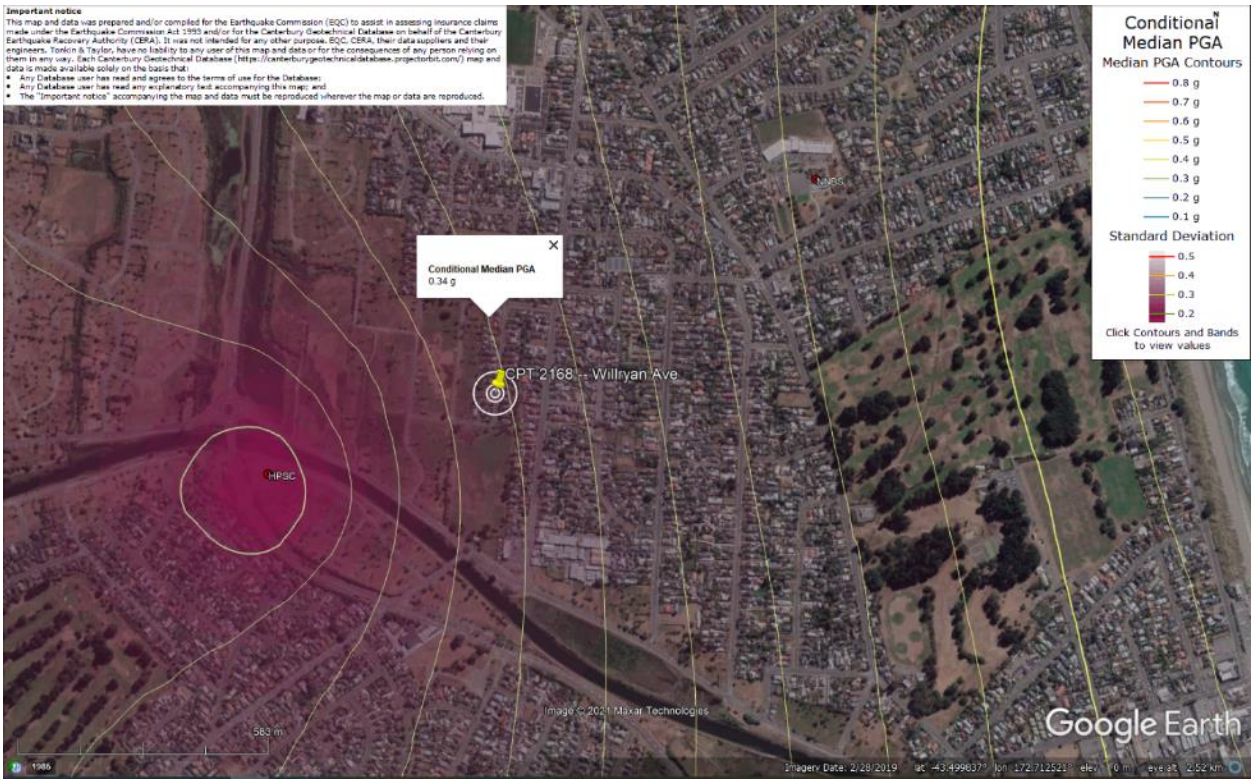

Figure 82: PGA for Dec-11 EQ (st. dev. = 0.300-0.325 ln units).

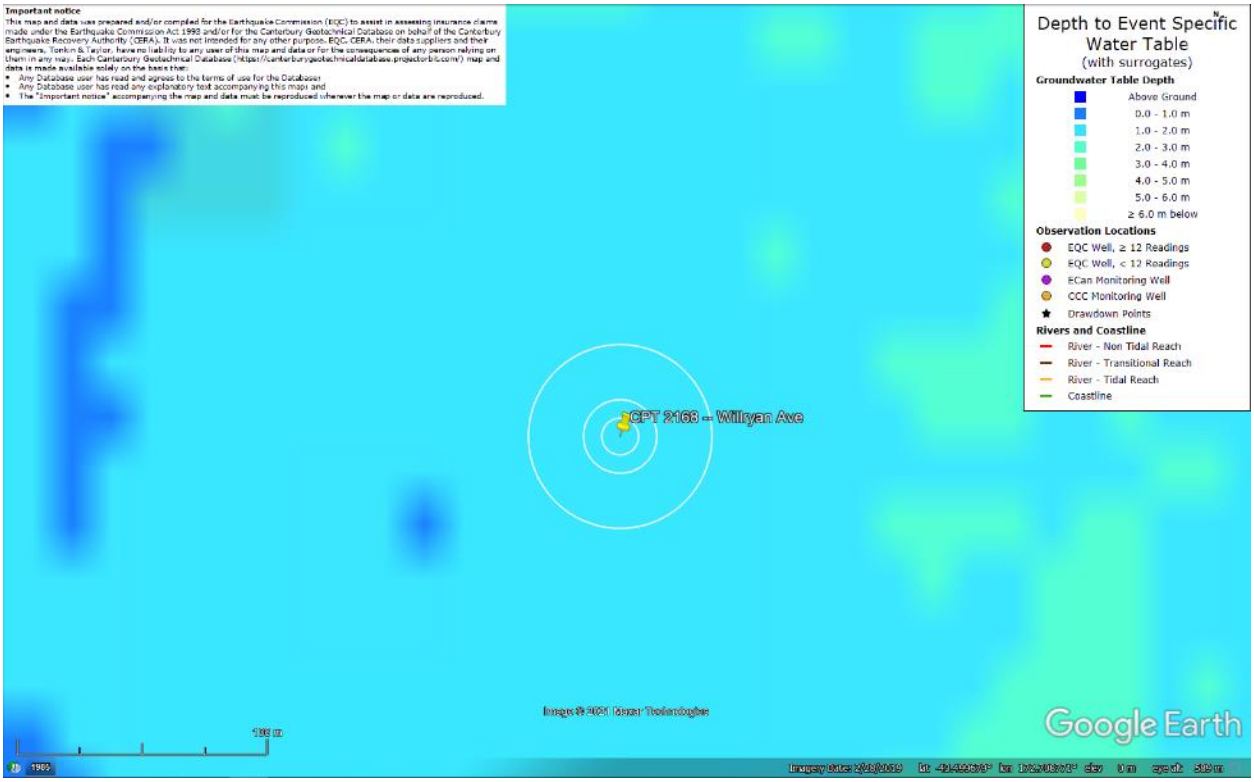

Figure 83: Depth to groundwater table for Sep-10 EQ.

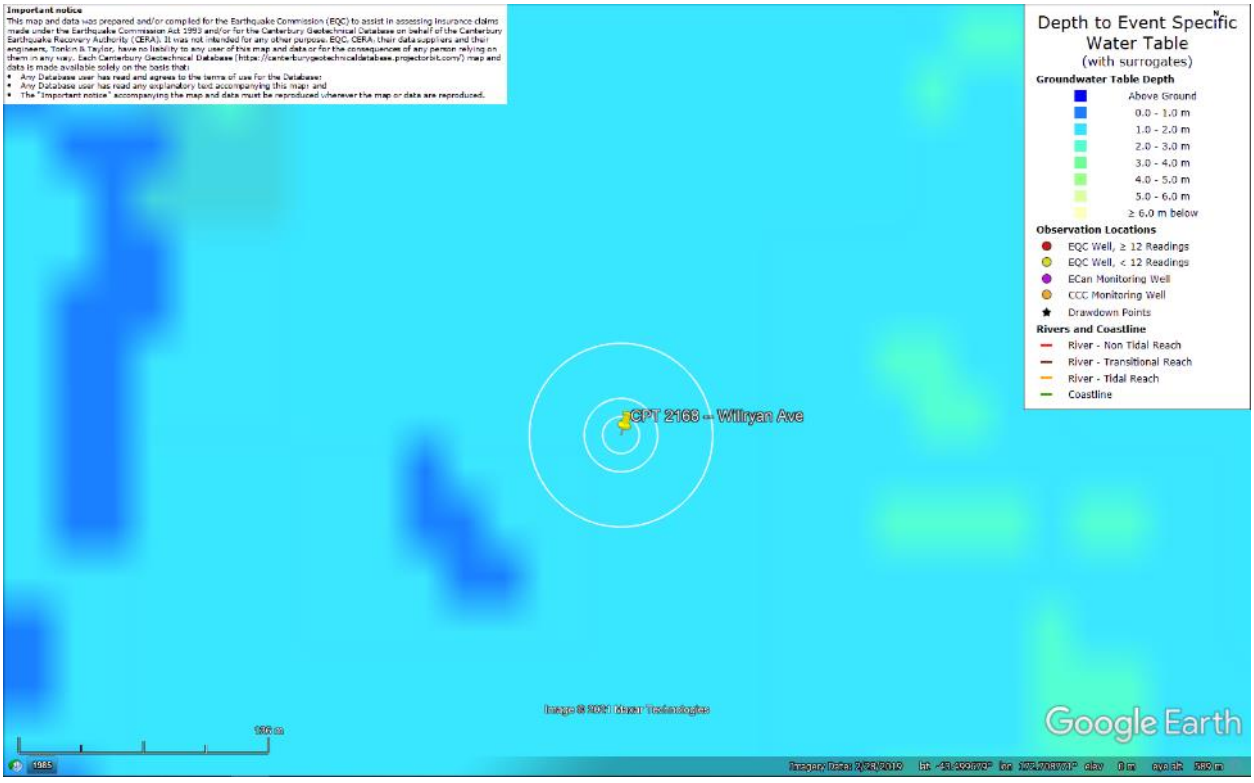

Figure 84: Depth to groundwater table for Feb-11 EQ.

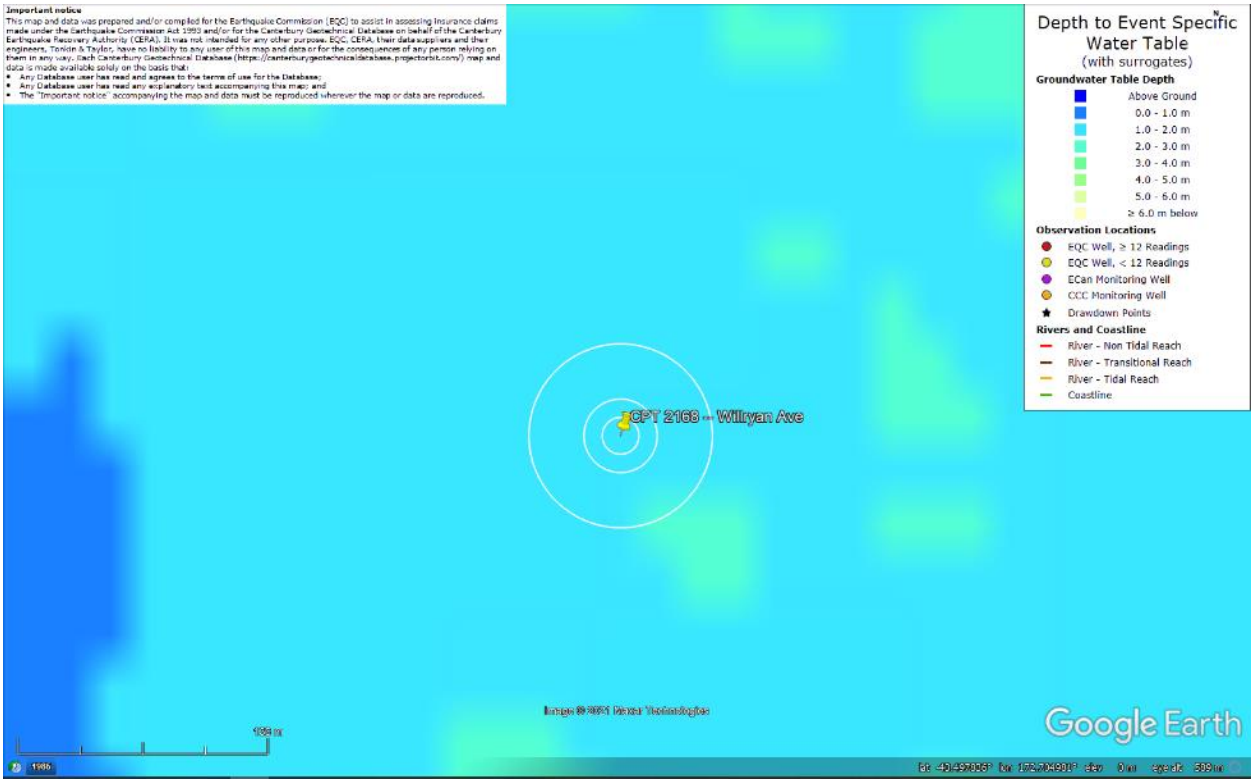

Figure 85: Depth to groundwater table for Jun-11 EQ.

Figure 86: Depth to groundwater table for Dec-11 EQ.

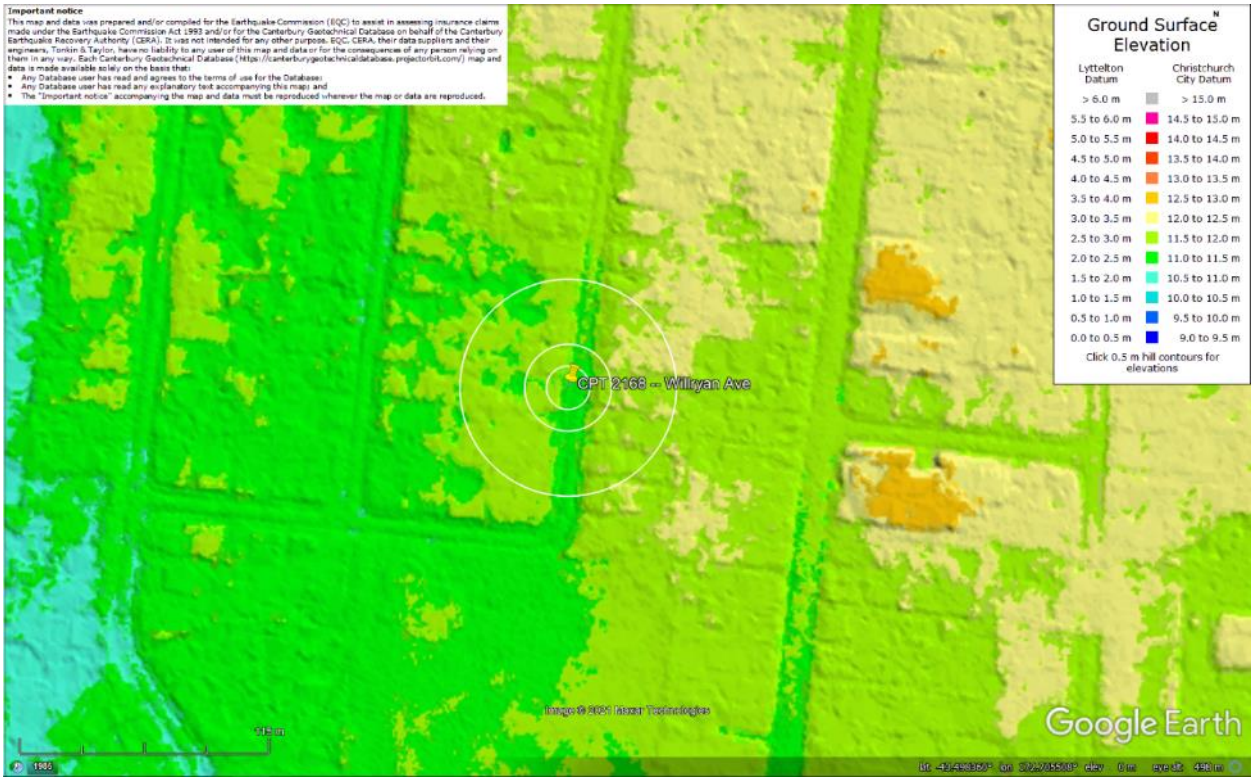

Figure 87: Ground surface elevation according to the Sep-2011 LiDAR survey; the properties are slightly elevated relative to the road (~0.5 m).

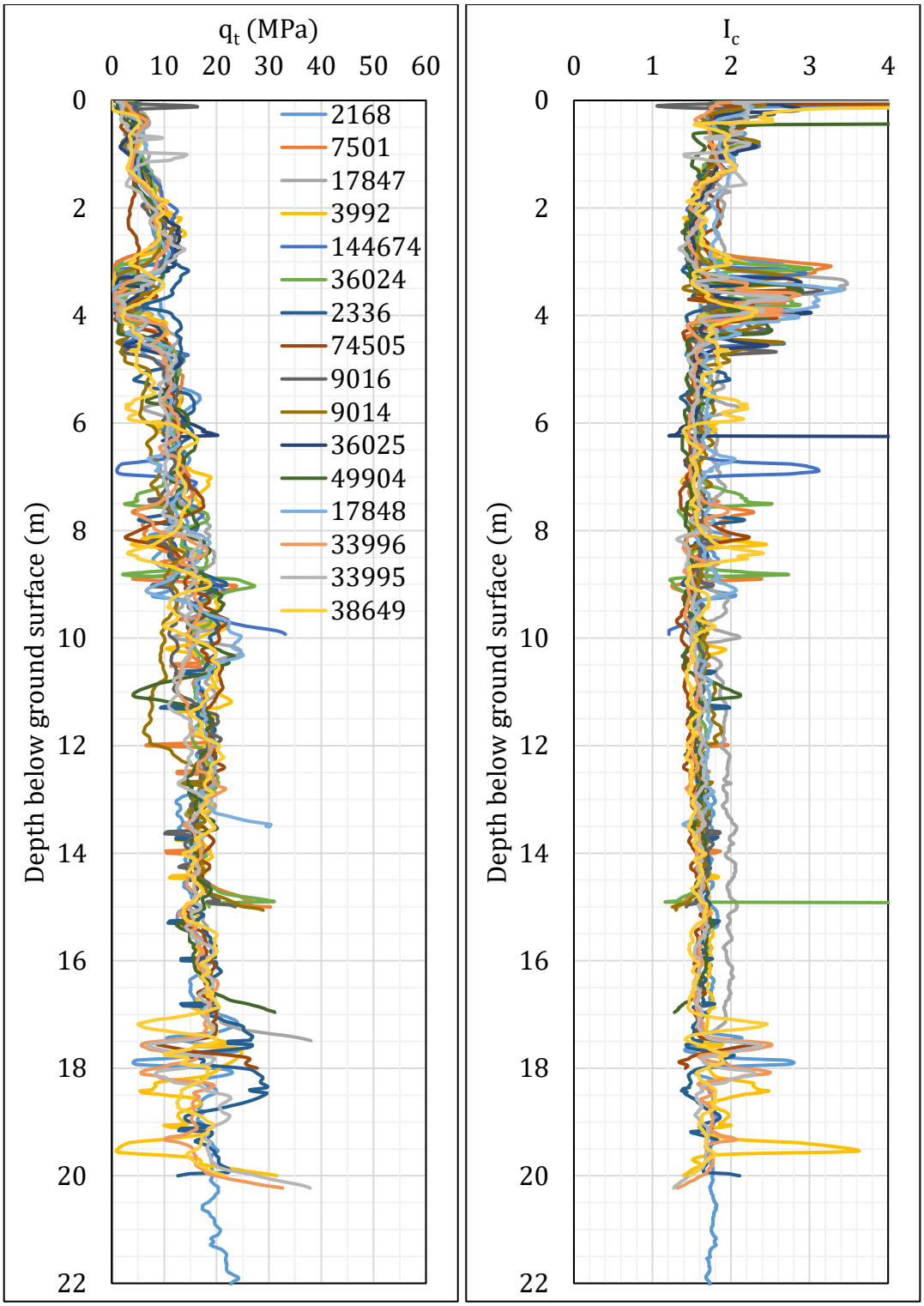

Figure 88: q_t and I_c profiles.

Note 6: The selection of CPTs for the area considered for settlement assessment (Figure 1) is based on the proximity of the CPTs to the considered areas. In accordance with that, the following table shows CPTs that were used for the volumetric settlement analysis in *Cliq v.3.0.3.2*, a CPT soil liquefaction software developed by GeoLogismiki. (The average volumetric settlements were reported in Table 8.)

Table 12: CPT profiles used in volumetric settlement analysis for areas selected for settlement assessment.

CPT ID No.	Patch A (20- and 50-m buffers)	Road (10-m buffer)	Road (20-m buffer)	Road (50-m buffer)
2168	✓	✓	✓	✓
7501	✓	✓	✓	✓
17847			✓	✓
3992			✓	✓
2339				✓
144674				✓
36024				✓
2336				✓
33995				✓
38649				✓
9014				
9016				
36025				
74505				
33996				
17848				
49904				

Note: CPTs 2168, 3992, and 2339 were used to compute the volumetric settlement for CPTs 7501, 17847, and 144674/36024, respectively, for the respective depth ranges: 15-20 m, 17.5-20 m, and 9.9/15-20 m.

Table 13: CPT-based results.

EQ Event	Parameter	CPT ID 2168	7501	17847	3992	2339	144674	36024	2336
Sep-10	S_{V1D} (mm)	4	20	1	18	13	2	8	11
	LSN	1	4	0	3	2	1	2	1
	LPI	0	0	0	0	0	0	0	0
	LPI_{ish}	0	0	0	0	0	0	0	0
	$D_{FS<1}$ (m)	undet.	undet.	undet.	undet.	undet.	undet.	undet.	undet.
Feb-11	S_{V1D} (mm)	88	76	14	65	74	33	64	46
	LSN	15	14	3	12	15	8	14	6
	LPI	6	7	1	5	6	4	6	3
	LPI_{ish}	1	4	1	3	4	2	4	0
	$D_{FS<1}$ (m)	2.31	2.66	3.63	2.82	1.52	3.26	3.16	4.98
Jun-11	S_{V1D} (mm)	11	34	4	29	24	8	21	14
	LSN	2	7	1	6	5	2	5	1
	LPI	0	2	0	1	1	0	1	0
	LPI_{ish}	0	1	0	0	1	0	1	0
	$D_{FS<1}$ (m)	undet.	7.82	undet.	3.44	3.5	undet.	3.51	undet.
Dec-11	S_{V1D} (mm)	82	80	13	66	81	42	70	49
	LSN	23	24	3	20	30	19	25	15
	LPI	5	8	1	5	8	5	6	3
	LPI_{ish}	3	7	1	4	8	5	6	2
	$D_{FS<1}$ (m)	0.71	0.72	3.63	1	0.98	0.73	0.71	0.88

Notes: $D_{FS<1}$ = Depth to the first liquefiable layer ($FS_L<1$) that is at least 200-mm thick, as determined by the Boulanger and Idriss (2016) liquefaction-triggering procedure (P_L=50%, C_{FC}=0.13, and $I_{c,cutoff}$ =2.6), and exported from *Cliq v.3.0.3.2*; undet. = the specified soil layer was not detected.

Table 13 (continued): CPT-based results.

		CPT ID					
EQ Event	Parameter	33995	38649	$\Delta_{CPT7501}$	$\Delta_{CPT17847}$	$\Delta_{CPT144674}$	$\Delta_{CPT36024}$
Sep-10	S_{V1D} (mm)	13	24	0	4	7	3
	LSN	2	4	0	0	0	0
	LPI	0	0	0	0	0	0
	LPI_{ish}	0	0	--	--	--	--
	$D_{FS<1}$ (m)	undet.	4.02	--	--	--	--
Feb-11	S_{V1D} (mm)	153	143	4	12	27	20
	LSN	27	23	1	1	2	1
	LPI	13	13	0	0	0	0
	LPI_{ish}	9	8	--	--	--	--
	$D_{FS<1}$ (m)	1.51	2.69	--	--	--	--
Jun-11	S_{V1D} (mm)	38	54	0	5	8	4
	LSN	8	10	0	0	1	0
	LPI	1	3	0	0	0	0
	LPI_{ish}	0	0	--	--	--	--
	$D_{FS<1}$ (m)	3.71	3.86	--	--	--	--
Dec-11	S_{V1D} (mm)	137	141	0	9	16	10
	LSN	30	36	0	1	1	1
	LPI	12	14	0	0	0	0
	LPI_{ish}	9	12	--	--	--	--
	$D_{FS<1}$ (m)	1.34	0.75	--	--	--	--

Notes: $D_{FS<1}$ = Depth to the first liquefiable layer ($FS_L<1$) that is at least 200-mm thick, as determined by the Boulanger and Idriss (2016) liquefaction-triggering procedure (P_L=50%, C_{FC}=0.13, and $I_{c,cutoff}$ =2.6), and exported from *Cliq v.3.0.3.2*; undet. = the specified soil layer was not detected; $\Delta_{CPT7501}$, $\Delta_{CPT17847}$, $\Delta_{CPT144674}$, and $\Delta_{CPT36024}$ indicate the amount of S_{V1D}, LSN, and LPI added to CPTs 7501, 17847, 144674, and 36024, respectively, due to the shallow penetration depths.

Note 7: Based on the borehole log (BH 2678, Figure 1), the groundwater table is at a depth of 3.1 m below the ground surface. The soil profile consists of (1) fine to medium sand, SP, to a depth of 2.7 m, (2) silt, ML, to a depth of 3.5 m, (3) fine to medium sand, SP, to a depth of 17.5 m, (4) silt, ML, to a depth of 17.8 m, and (5) fine to medium sand, SP, to a depth of 20 m. All soil layers are of the Christchurch formation.

Note 8: The ejecta-induced free-field settlement provided in Table 11 is an areal average settlement due to ejecta, which is based on the total settlement assessment area, A_T (provided in Table 9 and repeated in Table 14). However, the considered area was not always covered completely with ejecta; thus, it is important to provide the localized ejecta-induced settlement, too. The localized settlement due to ejecta is estimated using photographic evidence only as

$$S_{E,P\_localized} = \frac{V_E}{A_E}$$

where V_E is the total volume of ejecta within A_T and A_E is the total coverage area of ejecta within A_T. Please note that the areal ejecta-induced settlement provided in Table 14 as S_{E,P_areal} is the same as $S_{E,P}$ in Table 11, which was estimated as

$$S_{E,P\_areal} = S_{E,P} = \frac{V_E}{A_T}$$

where V_E is the total volume of ejecta within A_T and A_T is the total settlement assessment area.

Table 14a: Areal and localized ejecta-induced settlement estimates for Patch A (10-m buffer) based on photographic evidence.

Earthquake Event	A_T (m^2)	A_E (m^2)	V_E (m^3)	S_{E,P_areal} (mm)	$S_{E,P\_localized}$ (mm)
Sep-10	91.9	0	0	0	0
Feb-11	91.9	91.0	4.6-6.6	60±10	60±10
Jun-11	91.9	55.7	1.7-2.8	25±5	40±10
Dec-11	91.9	11.3	0.3-0.7	5±5	45±15

Notes: $S_{E,P\_areal} = S_{E,P}$ reported in Table 11 = areal ejecta-induced settlement; $S_{E,P\_localized}$ = localized ejecta-induced settlement; A_T = total settlement assessment area; V_E = total volume of ejecta within A_T; A_E = total area of ejecta within A_T; The estimates of both areal and localized ejecta-induced settlement are rounded to the nearest 5; Final plus/minus values are also rounded to the nearest 5.

Table 14b: Areal and localized ejecta-induced settlement estimates for Road (10-m buffer) based on photographic evidence.

Earthquake Event	A_T (m^2)	A_E (m^2)	V_E (m^3)	S_{E,P_areal} (mm)	$S_{E,P\_localized}$ (mm)
Sep-10	127	0	0	0	0
Feb-11	127	127	4.8-6.5	45±5	45±5
Jun-11	133	133	2.9-4.2	25±5	25±5
Dec-11	133	52.5	2.8-3.7	25±5	60±10

Notes: $S_{E,P\_areal} = S_{E,P}$ reported in Table 11 = areal ejecta-induced settlement; $S_{E,P\_localized}$ = localized ejecta-induced settlement; A_T = total settlement assessment area; V_E = total volume of ejecta within A_T; A_E = total area of ejecta within A_T; The estimates of both areal and localized ejecta-induced settlement are rounded to the nearest 5; Final plus/minus values are also rounded to the nearest 5.

Table 14c: Areal and localized ejecta-induced settlement estimates for Road (20-m buffer) based on photographic evidence.

Earthquake Event	A_T (m^2)	A_E (m^2)	V_E (m^3)	S_{E,P_areal} (mm)	$S_{E,P\_localized}$ (mm)
Sep-10	301	0	0	0	0
Feb-11	301	301	11.1-17.7	50±10	50±10
Jun-11	303	303	6.2-9.0	25±5	25±5
Dec-11	303	157	7.8-11.1	30±5	60±10

Notes: $S_{E,P\_areal} = S_{E,P}$ reported in Table 11 = areal ejecta-induced settlement; $S_{E,P\_localized}$ = localized ejecta-induced settlement; A_T = total settlement assessment area; V_E = total volume of ejecta within A_T; A_E = total area of ejecta within A_T; The estimates of both areal and localized ejecta-induced settlement are rounded to the nearest 5; Final plus/minus values are also rounded to the nearest 5.

Table 14d: Areal and localized ejecta-induced settlement estimates for Road (50-m buffer) based on photographic evidence.

Earthquake Event	A_T (m^2)	A_E (m^2)	V_E (m^3)	S_{E,P_areal} (mm)	$S_{E,P\_localized}$ (mm)
Sep-10	779	0	0	0	0
Feb-11	779	779	29.7-45.9	50±10	50±10
Jun-11	779	ND	ND	ND	ND
Dec-11	779	ND	ND	ND	ND

Notes: S_{E,P_areal} = $S_{E,P}$ reported in Table 11 = areal ejecta-induced settlement; $S_{E,P\_localized}$ = localized ejecta-induced settlement; A_T = total settlement assessment area; V_E = total volume of ejecta within A_T; A_E = total area of ejecta within A_T; The estimates of both areal and localized ejecta-induced settlement are rounded to the nearest 5; Final plus/minus values are also rounded to the nearest 5; ND = Not determined.

Summary 2:

- **The best estimate of the localized ejecta-induced free-field ground settlement at the Willryan Ave site for the SEP 2010, FEB 2011, JUN 2011, and DEC 2011 earthquake is 0 mm, 60±10 mm, 40±10 mm, and 45±15 mm, respectively.**
- **The best estimate of the localized ejecta-induced free-field settlement of the road at the Willryan Ave site for the SEP 2010, FEB 2011, JUN 2011, and DEC 2011 earthquake is 0 mm, 50±10 mm, 25±5 mm, and 60±10 mm, respectively.**